Journal of Asian Earth Sciences 84 (2014) 34–50

Contents lists available at ScienceDirect

Journal of Asian Earth Sciences

journal homepage: www.elsevier.com/locate/jseaes

Petrology and geochemistry of high-titanium and low-titanium mafic dykes from the Damodar valley, Chhotanagpur Gneissic Terrain, eastern India and their relation to Cretaceous mantle plume(s)

Rajesh K. Srivastava [a,*], Suresh Kumar [a,1], Anup K. Sinha [b], N.V. Chalapathi Rao [a]

[a] Centre of Advanced Study, Department of Geology, Banaras Hindu University, Varanasi 221 005, India
[b] Dr. K. S. Krishnan Geomagnetic Research Laboratory, Jhusi, Allahabad 211 505, India

ARTICLE INFO

Article history:
Available online 17 August 2013

Keywords:
Petrology
Geochemistry
Mafic dykes
Damodar valley
Eastern India
Kerguelen plume
Rèunion plume

ABSTRACT

The Damodar valley within the Chhotanagpur Gneissic terrain at the northern-most margin of the Singhbhum craton, eastern India, is perhaps the only geological domain in the entire Indian shield which hosts the early Cretaceous Rajmahal as well as the late Cretaceous Deccan igneous activities. A number of Cretaceous mafic dykes intrude the Gondwana sedimentary formations and are focus of the present study. One set of these dykes strike NNE to ENE, are very fresh and mainly exposed within the Jharia, Bokaro and Karanpura basins; whereas the other set of dykes (including the well-known Salma mega dyke) trend NW to NNW, intrude mainly the Raniganj basin and show meagre hydrothermal alteration. Majority of the samples from both these dyke groups display ophitic or sub-ophitic textures and are essentially composed of augite/titan augite and plagioclase. On the basis of petrographic and geochemical characteristics the NNE to ENE dykes are identified as high-Ti dolerite (HTD) dykes and the NW to NNW dykes are referred to as low-Ti dolerite (LTD) dykes. Apart from the first-order distinction on their titanium contents, both these groups also show conspicuous geochemical differences. The HTD dykes contain relatively high values of iron, and high-field strength elements than those from the LTD dykes with an overlapping MgO contents.

Although available field, paleomagnetic and limited geochronological data for most of the studied dykes suggests their emplacement during early Cretaceous period (110–115 Ma), the Salma dyke, dated to be of Deccan-age at ~65 Ma, is an exception. Geochemically all the studied samples show an undoubted plume-derived character but their unequivocal affinity to either the early Cretaceous Kerguelen (Rajmahal) or the late-Cretaceous Reunion (Deccan) plume is not straightforward since they share bulk-rock characteristics of rocks derived from both these plumes. Even though, the spatial and temporal association of the mafic dykes of present study with the Rajmahal Traps are suggestive of their linkage to the Kerguelen plume activity, robust geochronological and paleomagnetic constraints are clearly required to understand the relative contributions of the two Cretaceous mantle plumes in the genesis of the mafic igneous activity in this interesting domain.

1. Introduction

Large Igneous Provinces (LIPs) are defined as magmatic provinces with areal extents >1 Mkm^2, igneous volumes >0.1 Mkm^3 and maximum lifespan of ~50 Ma and that have intraplate tectonic settings or geochemical affinities, and are characterized by igneous pulse(s) of short duration (~1–5 Ma), during which a large proportion (>75%) of the total igneous volume has been emplaced (Coffin and Eldholm, 2005; Bryan and Ernst, 2008). Continental and oceanic flood basalts, volcanic rifted margins, giant dolerite dyke swarms, sill provinces and layered mafic–ultramafic intrusions can be an integral part of any LIP. Amongst these, mafic dyke swarms in shield areas, on account of their vertical depth and lateral extent provide the most complete record of short-lived, mantle-generated magmatic (LIPs) events through time and space (Halls, 1982; Fahrig, 1987; Halls and Fahrig, 1987; Parker et al., 1990; Baer and Heimann, 1995; Ernst and Buchan, 2001; Hanski et al., 2006; Bleeker and Ernst, 2006; Srivastava et al., 2010; Srivastava, 2011). In fact, record of mafic dyke swarms provides information on "the pulse of the Earth" beyond that related to mid-ocean ridge oceanic crust generation and record the rhythm of intraplate mantle melting events (Ernst and Buchan, 1997; Bleeker, 2004; Ernst et al., 2010). There is also an overall

* Corresponding author. Tel.: +91 9415812079.
E-mail address: rajeshgeolbhu@gmail.com (R.K. Srivastava).
[1] Present address: Geological Survey of India, Jabalpur 482 003, India.

1367-9120/$ - see front matter © 2013 Elsevier Ltd. All rights reserved.
http://dx.doi.org/10.1016/j.jseaes.2013.07.044

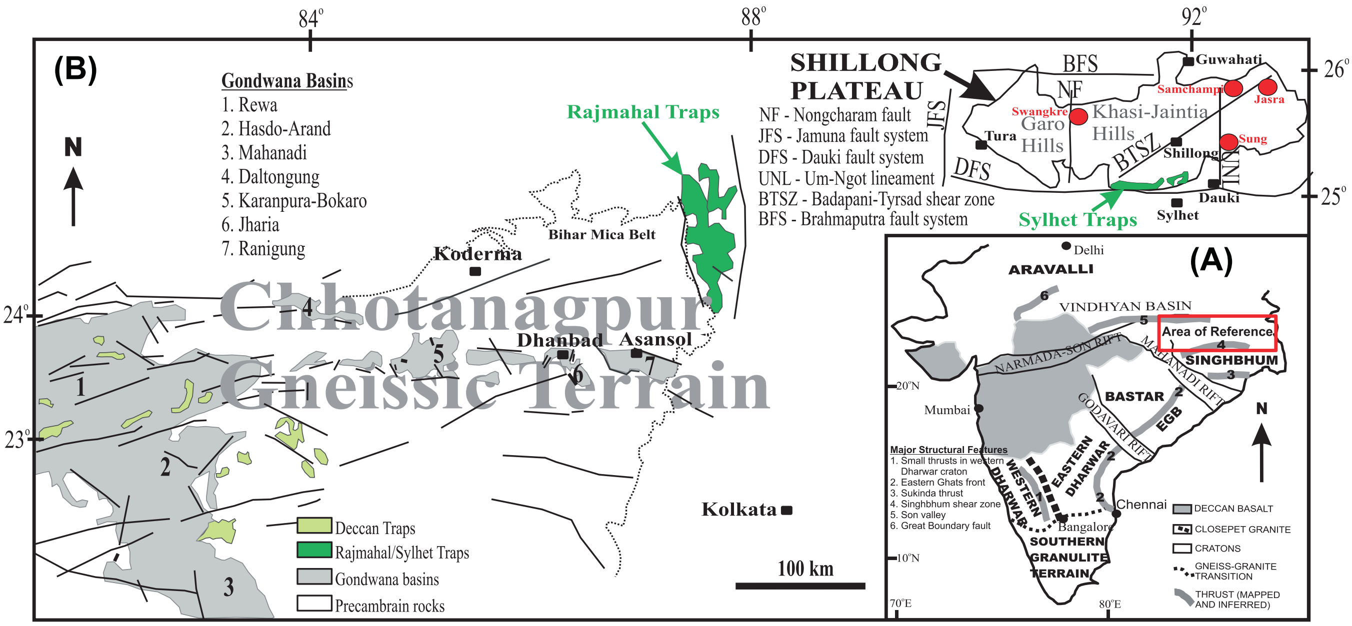

Fig. 1. (A) Major cratons and structural features of India (after Naqvi and Rogers, 1987). (B) Geological sketch map of northeastern India showing the locations of Late Cretaceous magmatic activity in the Damodar Valley, Rajmahal and Sylhet Traps and on the Shillong Plateau (modified after Kent et al., 1997; Melluso et al., 2012).

agreement that mantle plumes to be the source for many or all of the LIPs (Ernst and Buchan, 2001; Foulger, 2010).

The Indian shield is broadly an assembly of dominantly Archean–Paleoproterozoic cratonic blocks and predominantly Meso-neoproterozoic mobile belts with Archean protoliths (Naqvi et al., 1974; Naqvi and Rogers, 1987; Ramakrishnan and Vaidyanadhan, 2010). Mafic dykes and dyke swarms of variable compositions, different structural orientations and with different emplacement periods are very conspicuous in the entire Indian shield (Murthy, 1987; Devaraju, 1995; Srivastava et al., 2008a; Srivastava et al., 2008b; Srivastava and Ahmad, 2008, 2009; Srivastava, 2011). Although mafic dykes are more common in Archaean cratons, early- and late-Cretaceous mafic and alkaline igneous activity (represented by mafic dykes, volcanic, alkaline plugs and ultramafic–carbonatite complexes of the Deccan volcanic province, Rajmahal–Sylhet traps and Shillong plateau), is also well-recorded from the Indian Shield (Athavale and Verma, 1970; Karkare and Srivastava, 1990; Storey et al., 1992; Kent et al., 1996; Kent et al., 1997; Kent et al., 1998; Kent et al., 2002; Srivastava and Sinha, 2004a,b, 2007; Paul, 2005; Srivastava et al., 2005; Srivastava et al., 2008a; Srivastava et al., 2008b; Srivastava et al., 2009; Ray et al., 2007; Misra, 2008; Patil and Arora, 2008; and references therein). These early- and late-Cretaceous igneous events have been widely attributed to plume tectonics (Foulger, 2010 and references therein) involving either the Réunion plume in case of late-Cretaceous Deccan Traps (Courtillot et al., 1988; White and McKenzie, 1989; Chalapathi Rao and Lehmann, 2011; Chalapathi Rao et al., 2011) or the Kerguelen plume in case of early-Cretaceous Rajmahal–Sylhet Traps (Kent, 1991; Baksi, 1995; Coffin et al., 2002; Kent et al., 1997, 2002; Srivastava and Sinha, 2007). Probably the Damodar valley is the only domain in the Indian shield which evidenced the early Cretaceous Rajmahal as well as the late Cretaceous Deccan igneous activities.

This paper presents new petrological and geochemical data on wide-spread Cretaceous mafic dykes intruding the Gondwana sedimentary basins in the Damodar valley within the Chhotanagpur Gneissic Terrain (CGT) at the northern-most margin of the Singhbhum craton (Figs. 1 and 2). There is a paucity of petrological and geochemical information available on these dykes (Kent et al., 1997; Paul, 2005) compared to their Precambrian counterparts elsewhere from other Indian cratons. Likewise, palaeomagnetic data on these dykes is also limited (Athavale and Verma, 1970 and Patil and Arora, 2008). The genetic association of these Cretaceous mafic dykes is debated with regard to their linkage with the Deccan or Rajmahal–Sylhet Traps since both of these events have been documented from the Damodar valley and the CGT domain (Fig. 1B).

One of these mafic dykes, viz. Salma dyke, has been dated by Ar–Ar method to be of 65.4 ± 0.3 Ma (Kent et al., 2002) which is close to the age of the main eruption of the Deccan volcanism (see Chenet et al., 2007). On the other hand, a number of NE trending mafic dykes, which are exposed within the Precambrian rocks around Koderma (see Fig. 2B), have K–Ar ages ∼110 Ma (Agarwal and Rama, 1976; Kent et al., 1997). Subsequently, Kent et al. (1997, 2002) have dated one of these Koderma dolerite dykes by Ar–Ar method which yielded a plateau age at 115.3 ± 0.4 Ma. Another dolerite dyke exposed around Kalidaspur area of the Raniganj basin gave Ar–Ar plateau age at 112.5 ± 0.5 Ma (Kent et al., 2002) (see Table 1). These ages are closer to Kerguelen plume-related early Cretaceous igneous activities (Coffin et al., 2002; Kent et al., 2002; Srivastava and Sinha, 2007). The main objectives of this study are to investigate (i) whether all the studied dykes are of co-genetic in nature or represent different episodes, related to Deccan and/or Rajmahal–Sylhet events, and (ii) evaluate their relationship, if any, vis-a-vis the plume tectonics.

2. Geological setting

The eastern part of the Indian shield consists mainly of Singhbhum craton, Chhotanagpur Gneissic Terrain (CGT) and Shillong plateau (see Figs. 1 and 2). There is much debate over exact relationship between Singhbhum craton and Chhotanagpur Gneissic Terrain (CGT); whilst some workers regard CGT as a mobile belt and constitutes a distinct terrane (Ghose, 1983; Mukhopadhyay, 1988; Mahadevan, 2002; Ghose and Chatterjee, 2008 and references therein), others regard it to be a cratonised mobile belt (Naqvi and Rogers, 1987; Kumar and Ahmad, 2007; Sharma, 2009; Srivastava et al., 2009, 2012). Sharma (2009) discussed this

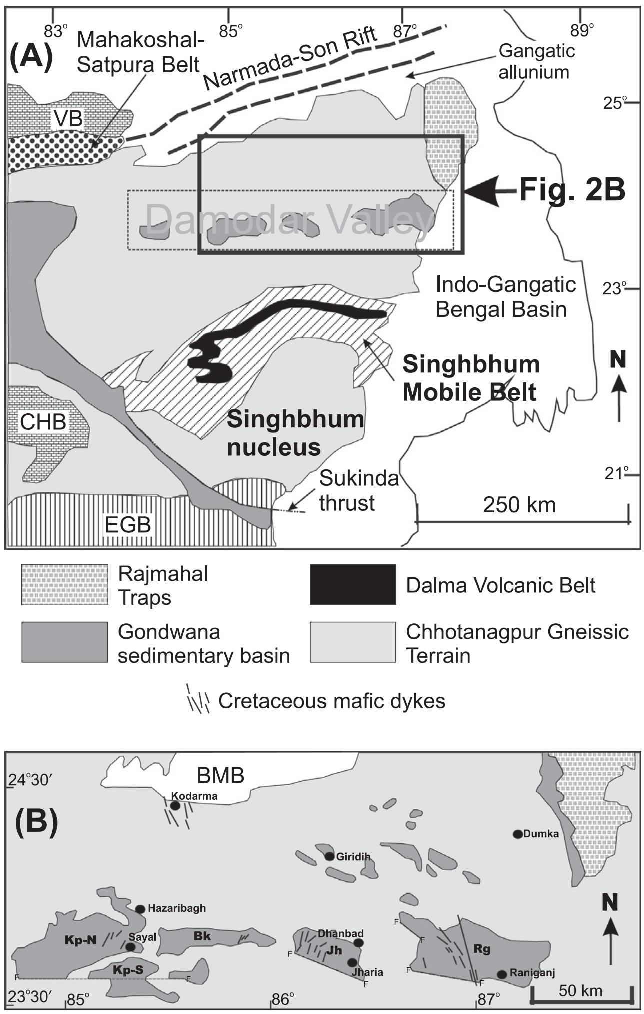

Fig. 2. (A) Geological map of the Chhotanagpur Gneissic Terrain (CGT) and distribution of Gondwana basins in the Damodar Valley, Eastern India (modified after Acharyya, 2003; Srivastava et al., 2012). VB: Vindhyan basin; CHB: Chhattisharh basin; EGB: Eastern Ghats Belt. (B) Simplified geological map of part of CGT showing Damodar valley Gondwana sedimentary basins and Rajmahal basalts (modified after Mahadevan, 2002). BMB: Bihar mica belt; Jh: Jharia; Rg: Raniganj; Bk: Bokaro; Kp-N: North Karanpura; Kp-S: South Karanpura.

issue at length and stated many geological reasons that questioned its mobile belt nature. There is no explanation available in literature that can explain the absence of a crustal block that had collided against the Singhbhum craton more than once to produce North Singhbhum Fold Belt as well as the CGT (Sharma, 2009). Sharma (Op. cit) also noted that the CGT has an Archaean antiquity whose convergence with the Singhbhum craton in the south gave rise to the Singhbhum mobile belt and medium-grade enclaves of metasediments and basic rocks exclude its mobile belt nature. Misra (2006) has reported a number of magmatic–metamorphic events in the CGT at ~2.3 Ga, 1.6–1.5 Ga and 0.9 Ga. Besides these features, there are other features observed in the CGT which support its cratonic nature. These includes – (i) occurrences of spinifex textured komatiite within the CGT, near Daltonganj (Bhattacharya et al., 2010); (ii) presence of potassic intrusives with petrological and geochemical affinities to predominantly cratonic magmas such as orangeites, lamproites and aillikites – (Srivastava et al., 2009) and (iii) Mesoproterozoic metabasite rocks and amphibolites dykes respectively exposed south and north of the Damodar valley show their emplacement in an extensional tectonic regime of intracratonic setting (Ghose et al., 2005; Kumar and Ahmad, 2007). Five major intra-continental rift/shear zones, mostly trend in ENE–WSW to E–W and which controlled the magmatism in the CGT, have been identified (Ghose and Chatterjee, 2008). Therefore, it is believed that Singhbhum craton consists of Singhbhum nucleus, Chhotanagpur Gneissic Terrain and Singhbhum mobile belt; latter separates the former two blocks (Fig. 2; cf. Naqvi and Rogers, 1987). Polyphase deformation, metamorphism and magmatism are conspicuous features of the CGT (Ghose, 1983; Mahadevan, 2002).

Mafic dykes of different ages (Mesoproterozoic to Cretaceous) are well exposed in the CGT. A number of ENE–WSW to E–W trending Mesoproterozoic mafic dykes intrude the basement gneisses of the CGT; but these dykes are not found in the massif anorthosite and granite plutons (Ghose, 1983; Mahadevan, 2002; Ghose et al., 2005; Kumar and Ahmad, 2007; Ghose and Chatterjee, 2008; Srivastava et al., 2012). On the other hand, not much petrological and geochemical database is available for the Cretaceous mafic dykes. Kent et al. (1997) have presented petrological, geochemical and isotopic data for mafic dykes from the Raniganj (including the ~65 Ma Salma dyke), Jharia and Koderma areas, whereas Paul (2005) has presented geochemical data for a 45–55 km long and 50–100 m wide, NNW trending ~65 Ma Salma dyke intruding the Raniganj coal field as well the Precambrian basement of the CGT. These Cretaceous mafic dykes, mostly very fresh and doleritic in nature, essentially intrude the Gondwana sedimentary (coal) basins of the Damodar valley (Fig. 2B). A number of mafic dykes are also encountered from the Bokaro and Karanpura areas (Fig. 2B), however most of them are extremely altered. There are other mafic dykes with similar trend (NW to NNW) to that of the Salma are also reported from the Raniganj basin. They vary in length between 100 and 600 m and width between 10 and 50 m. Another set of mafic dykes having an altogether different trend (NNE to ENE) are reported to cut across Jharia basin but not the adjacent Precambrian basement. The biggest dyke of this group is ~6 km in length and occurs near Madhuban. Others vary in length from 50 m to 500 m and width of 10 m to 20 m. A number of ~110–115 Ma NE trending mafic dykes are also reported to cut the Precambrian rocks around Koderma (see Fig. 2B) (Agarwal and Rama, 1976; Kent et al., 1997, 2002). Thus, the field observations bring out two sets of Cretaceous mafic dykes; one trending in NW to NNW (also includes the Salma dyke) and other in NNE to ENE direction.

Cretaceous igneous activity is also very conspicuous in northeastern Indian shield. This is represented by the Rajmahal and Sylhet tholeiitic basalts (traps) and mafic dykes and a number of ultramafic–alkaline–carbonatite igneous complexes of the Shillong plateau (Storey et al., 1992; Srivastava and Sinha, 2004a, 2007; Srivastava et al., 2005, 2009; Mallikharjuna Rao, 2002; Kent et al., 1997, 1998, 2002; Srivastava et al., 2012) (see Fig. 1B). All these magmatic activities of the region are also thought to be associated to the Kergulen plume activity (Coffin et al., 2002; Kent et al., 2002; Srivastava and Sinha, 2007). Likewise, N–S trending Cretaceous mafic dykes, emplaced within the Precambrian rocks, are also well exposed in the Swangkre-Rongmil region of the Shillong plateau and are show very close geochemical similarities with the mafic rocks derived from the Kerguelen mantle plume (Srivastava and Sinha, 2004b).

3. Petrography

As dyke alteration is more at contact margins, most samples were collected from middle portion as far as possible of the dykes with massive-homogenize characteristics and free from any vein, alteration or pegmatitic texture to minimize any contamination. Most of the studied mafic dyke samples, collected from different Cretaceous mafic dykes, are medium to coarse-grained and doleritic in nature (Fig. 3); samples collected from close to the dyke

Table 1
Available radiometric and palaeomagnetic ages on the mafic dykes, traps, alkaline rocks and carbonatites from the eastern and north-eastern Indian shield.

	Area/unit	Age in Ma	Method	Reference	Remarks
Mafic dykes from the Chhotanagpur gneissic terrain and Damodar valley basins					
1.	Kalidaspur, Raniganj basin	112.5 ± 0.5	Ar–Ar[a]	Kent et al. (2002)	This dyke is emplaced just adjacent to the Salma dyke having same trend
2.	Koderma	115.3 ± 0.4	Ar–Ar[a]	Kent et al. (2002)	Trends in NW direction and emplaced within the Chhotanagpur Gneissic Terrain
3.	Asansol, Salma dyke, Raniganj	65.4 ± 0.3	Ar–Ar[a]	Kent et al. (2002)	
4.	Salma dyke, Salma	~117 Ma	Palaeomagnetic age	Patil and Arora (2008)	This samples is from the Salma dyke but giving Rajmahal basalt age
Tholeiite basaltic traps of eastern and north-eastern India					
1.	Rajmahal basalt	116.2 ± 0.6	Ar–Ar[a]	Pringle et al. (1994)	
2.	Rajmahal basalt	117.5 ± 0.5	Ar–Ar[a]	Baksi (1995)	
3.	Rajmahal basalt	118.2 ± 0.3	Ar–Ar[a]	Coffin et al. (2002)	
4.	Dhanbad, Rajmahal basalt	117.9 ± 0.4	Ar–Ar[a]	Kent et al. (2002)	Kent et al. (2002) also recorded a number of younger ages, between 109 Ma and 102 Ma, for Rajmahal basalts but kept them in less reliable age category.
5.	Mirza Cauki, Rajmahal basalt	117.4 ± 0.5	Ar–Ar[a]	Kent et al. (2002)	
6.	Galsi, Bengal basin borehole basalt	117.1 ± 0.4	Ar–Ar[a]	Baksi (1995)	
7.	Jalangi, Bengal basin borehole basalt	116.9 ± 2.3	Ar–Ar[a]	Baksi (1995)	
8.	Sylhet trap	110 ± 3	K–Ar	Sarkar et al. (1996)	
Ultramafic/ultrapotassic intrusive in the Damodar valley					
1.	Orangeites	113.5 ± 0.5	Ar–Ar laser probe	Kent et al. (1998)	
2.	Lamprophyre from Damodar valley	114.9 ± 0.3	Ar–Ar[a]	Coffin et al. (2002)	
Alkaline-carbonatite complexes, Shillong plateau					
1.	Sung valley pyroxenite and phlogopite from carbonatite	107.2 ± 0.8	Ar–Ar[a]	Ray et al. (1999)	
2.	Sung valley complex	106 ± 11	Rb–Sr	Ray et al. (2000)	
3.	Sung valley: perovskite from ijolite	115.1 ± 5.1	U–Pb	Srivastava et al. (2005)	
4.	Jasra: zircon and baddeleyite from gabbro	105.2 ± 0.5	U–Pb	Heaman et al. (2002)	
5.	Swangkre lamprophyre	107 ± 4	K–Ar	Sarkar et al. (1996)	

[a] Plateau ages.

margins are fine-grained. Mafic dykes trending in NNE to ENE directions, and mainly exposed within the Jharia basin, are very fresh and rarely any alteration is noticed. These mafic dykes mainly show ophitic or sub-ophitic textures (Fig. 3A–C), however, at places, some coarser samples also exhibit hypidiomorphic texture. They essentially contain augite/titan augite and plagioclase as major constituents, however most interesting feature observed in these samples is that they contain sufficient amount of rutile (up to 8 vol%) and ilmenite (up to 7 vol%) (Fig. 3B and C). As both rutile (TiO_2) and ilmenite ($FeTiO_3$) are titanium rich, this variety is classified as Ti-rich dolerites. Other minerals present in minor to subordinate proportions include biotite, zircon, titanite and apatite. No hypersthene or olivine is noticed in this type.

NW to NNW trending the Salma mafic dyke and other similar dykes of same trend show ophitic or sub-ophitic (Fig. 3D and E) or hypidiomorphic textures and essentially contain augite/titan augite and plagioclase as major constituents. These are relatively coarser than the first variety. They also contain sufficient amount of ilmenite (up to 10 vol%), however rutile is rare. In many of these samples plagioclase is altered and show clouding (Fig. 3D and E). This is very likely due to saussuritization of plagioclase grains as a result of late-hydrothermal activities. Fine-grained samples, collected from margin of the samples, of both these types show porphyritic texture (Fig. 3F). We classify this variety as low-Ti dolerites.

4. Analytical techniques

More than 60 samples from distinct Cretaceous mafic dykes from the CGT were collected for detailed petrographic and geochemical studies. Thirty-two fresh samples (twenty-two from the NNE to ENE trending and ten from the NW to NNW trending mafic dykes), devoid of any possible alterations were selected for whole rock major and trace element chemical analyses. All analyses were done at the Activation Laboratories Ltd., Ancaster, Ontario, Canada. An inductively coupled plasma (ICP) spectrometry (Model: Agilent 735) was used to analyze major elements by lithium metaborate/tetraborate fusion method and accuracy is much better than 1–2%, whereas, an inductively coupled plasma mass spectrometry (ICP-MS; Model: Perkin Elmer Sciex ELAN 9000) was used to determine trace element concentrations and at 100× the detection limit, accuracy is better than 5%. Several standards, such as NIST 694, SY-4, BIR-1, W-2A, and WMG-1, were run to check accuracy and precision. The analytical procedure is detailed by Gale et al. (1997) and details available in the Activation Laboratories Ltd website (http://www.actlabs.com). The entire chemical analyses together with CIPW normative compositions, calculated by SINCLAS computer program (Verma et al., 2002), of different dolerite types are presented in Tables 2 and 3.

Fig. 3. Photomicrographs of the studied dolerite samples (A–C and F from the HTD and D–E from the LTD). Ophitic/sub-ophitic textures are clearly visible in most of the photographs except 'F' which shows porphyritic texture. Rutile and ilmenite are present in sufficient amount in the HTD type (see B and C). Width of each photograph is equivalent to 5 mm.

5. Geochemistry

Henceforth, we prefer to refer the mafic dykes trending in NNE to ENE direction and containing higher modal proportion of titanium rich minerals (rutile and ilmenite) as high-Ti dolerite (HTD) dykes and those trending in NW to NNW and having relatively lesser amount of titanium-rich mineral phases as low-Ti dolerite (LTD) dykes. This division is explicitly illustrated in the MgO–TiO_2 plot (see Fig. 5A) presented later in this section. From the geochemical data of the studied mafic dyke samples it is observed that all of them show very limited geochemical variation (see Tables 2 and 3, respectively). The CIPW normative compositions of both the types are quite similar with a quartz normative character; however normative hypersthene and ilmenite are slightly higher in the HTD samples than the LTD samples (see Tables 2 and 3). The HTD dykes also have a comparatively lower Mg# (average ~43) than the LTD samples (average ~55). The SINCLAS computer program (Verma et al., 2002) and the TAS diagram (Fig. 4: Irvine and Baragar, 1971; Le Maitre, 2002) classify the HTD dyke samples as sub-alkaline basalt, whereas the LTD dyke samples show sub-alkaline basaltic andesite characteristics. Geochemical characteristics of the studied samples are further examined on a number of variation diagrams (Fig. 5A). In all these plots, both these groups show very distinct geochemical characteristics. In general, the HTD dykes show higher concentrations of Fe_2O_3, TiO_2, and P_2O_5 and lower values of SiO_2, alkalis, and Al_2O_3 than those from the LTD dykes. These geochemical observations very likely portray different genetic histories for both types. Fig. 5B presents variations of Cr and selected large-ion lithophile elements (LILEs); except for Ba, other elements mimic the same aspects as observed from the major oxides. Scattered behavior of Ba, a mobile element, is probably due to late hydrothermal alterations as saussuritization in plagioclase grains is observed in many samples.

High-field strength elements (HFSEs) are generally considered to be the best proxies to study samples that suffered from post-magmatic processes like low-grade metamorphism and hydrothermal alterations owing to their relatively immobile nature (Pearce and Cann, 1973; Floyd and Winchester, 1978; Rollinson, 1993; Jochum and Verma, 1996). Therefore, variations of some of HFSEs

Table 2
Whole rock major oxides (wt%), CIPW Normative compositions and trace elements (ppm) of Cretaceous Ti-rich mafic dykes from the Chhotanagpur Gneissic Terrain, Singhbhum craton, eastern India.

GPS Data ↓	1 JH5/18	2 JH5/19	3 JH6/14	4 JH6/15	5 JH6/17	6 JH6/18	7 JH6/21	8 JH6/23	9 JH6/25	10 JH6/35	11 JH8/4
Latitude	23°45′29″	23°45′55″	23°46′57″	23°47′07″	23°47′07″	23°45′04″	23°45′09″	23°44′55″	23°44′50″	23°44′24″	23°44′54″
Longitude	86°11′02″	86°11′12″	86°14′21″	86°14′44″	86°14′28″	86°11′20″	86°11′40″	86°11′05″	86°11′37″	86°11′18″	86°10′35″
Major oxides (wt%)											
SiO_2	48.68	48.19	48.65	48.85	48.81	48.63	48.71	48.68	48.61	49.26	48.39
TiO_2	2.94	2.96	2.79	2.81	2.89	2.88	2.90	2.86	2.83	2.81	2.56
Al_2O_3	12.85	12.67	13.88	13.32	13.20	13.30	13.17	13.30	13.60	13.11	12.9
Fe_2O_3	16.38	16.21	15.81	16.12	16.68	16.48	16.81	16.56	15.74	16.21	16.35
MnO	0.23	0.23	0.22	0.22	0.23	0.22	0.23	0.23	0.21	0.22	0.22
MgO	5.31	5.37	5.12	5.48	5.22	5.28	5.18	5.30	5.15	5.33	5.47
CaO	9.81	9.71	9.33	9.39	9.34	9.27	9.29	9.34	9.51	9.67	9.92
Na_2O	2.31	2.29	2.36	2.30	2.30	2.32	2.35	2.35	2.38	2.33	2.24
K_2O	0.61	0.68	0.70	0.66	0.66	0.68	0.67	0.65	0.57	0.56	0.50
P_2O_5	0.30	0.31	0.30	0.30	0.33	0.31	0.33	0.31	0.31	0.30	0.32
LOI	0.63	0.54	0.72	1.06	0.61	0.70	0.41	0.40	1.03	0.34	0.47
Total	100.05	99.16	99.88	100.51	100.27	100.07	100.05	99.98	99.94	100.14	99.34
Mg#	43.11	43.64	43.08	44.28	42.25	42.82	41.87	42.80	43.34	43.46	43.88
TAS Class[na]	SAB	SAB	SAB	SAB	SAB	SAB	SAB	SAB	SAB	SAB	SAB
CIPW norm											
Q	2.53	2.16	2.38	2.56	2.80	2.48	2.49	2.30	2.70	3.14	2.28
Or	3.68	4.13	4.23	3.98	3.97	4.10	4.03	3.91	3.45	3.36	3.03
Ab	19.94	19.93	20.42	19.84	19.81	20.04	20.25	20.26	20.64	20.03	19.42
An	23.35	22.92	25.77	24.54	24.17	24.36	23.83	24.27	25.36	24.04	24.51
Di	20.25	20.43	16.29	17.44	17.37	17.11	17.45	17.41	17.43	18.93	19.82
Hy	20.16	20.23	21.21	21.85	21.77	21.88	21.7	21.87	20.62	20.73	21.46
Mt	3.69	3.69	3.57	3.63	3.75	3.72	3.78	3.73	3.57	3.64	3.70
Il	5.70	5.77	5.42	5.45	5.59	5.58	5.61	5.53	5.51	5.42	5.02
Ap	0.71	0.74	0.71	0.71	0.78	0.73	0.78	0.73	0.74	0.71	0.76
Trace elements (ppm)											
Cr	-	-	80	80	70	90	70	80	90	100	110
Ni	-	-	70	70	60	70	60	60	60	80	90
Rb	-	-	16	15	15	15	16	15	13	14	14
Ba	165	516	694	767	273	420	666	596	212	150	411
Sr	200	135	218	200	208	201	212	214	209	208	196
Nb	-	-	13	12	13	13	13	13	12	12	12
Ta	-	-	1.0	0.9	1.1	1.0	1.0	1.0	1.0	0.8	0.9
Zr	190	192	164	165	180	169	179	169	169	165	123
Hf	-	-	4.6	4.6	5.1	4.8	4.8	4.9	4.9	4.4	4.1
Y	39	40	36	37	40	38	40	38	37	37	35
Ga	-	-	24	23	23	24	24	24	23	24	23
Th	-	-	1.8	1.7	1.9	1.8	1.8	1.7	1.8	1.6	1.6
U	-	-	0.5	0.5	0.5	0.5	0.5	0.5	0.5	0.5	0.4
La	-	-	16.20	15.30	17.10	15.90	16.10	16.30	16.10	15.20	14.20
Ce	-	-	38.20	36.10	40.20	37.70	38.20	38.60	38.30	37.10	34.10
Pr	-	-	5.09	4.89	5.40	5.03	5.17	5.21	5.20	4.87	5.00
Nd	-	-	23.80	23.20	25.90	23.50	24.80	24.50	24.30	23.10	21.90
Sm	-	-	6.30	6.30	6.80	6.50	6.70	6.60	6.50	5.80	5.70
Eu	-	-	2.22	2.13	2.26	2.22	2.27	2.29	2.27	2.23	1.96
Gd	-	-	6.40	6.30	7.00	6.70	6.80	6.90	6.70	6.80	6.60
Tb	-	-	1.20	1.20	1.30	1.30	1.30	1.30	1.20	1.20	1.10
Dy	-	-	7.40	7.30	8.10	7.70	8.00	8.00	7.60	7.10	6.60
Ho	-	-	1.40	1.40	1.50	1.50	1.50	1.50	1.40	1.30	1.40
Er	-	-	4.00	3.90	4.30	4.10	4.10	4.20	4.00	3.80	3.90
Tm	-	-	0.56	0.56	0.62	0.60	0.60	0.60	0.59	0.56	0.57
Yb	-	-	3.50	3.70	3.90	3.80	3.70	3.80	3.80	3.50	3.40
Lu	-	-	0.52	0.54	0.58	0.53	0.56	0.54	0.53	0.51	0.49
Nb/La	-	-	0.80	0.78	0.76	0.82	0.81	0.80	0.75	0.79	0.85
Nb/Ce	-	-	0.34	0.33	0.32	0.34	0.34	0.34	0.31	0.32	0.35
La^N/Lu^N	-	-	3.23	2.94	3.06	3.11	2.98	3.13	3.28	3.09	3.01
La^N/Sm^N	-	-	1.62	1.53	1.58	1.54	1.51	1.55	1.56	1.65	1.57
GPS Data ↓	12 JH8/5	13 JH8/6A	14 JH8/8A	15 JH8/8B	16 JH8/8C	17 JH8/10	18 JH8/11	19 JH8/JD4	20 JH8/JD5	21 JH8/PT1	22 JH8/PT2
Latitude	23°44′05″	23°41′23″	23°41′04″	23°41′012	23°41′33″	23°46′34″	23°46′51″	23°47′19″	23°47′19″	23°40′28″	23°40′28″
Longitude	86°10′54″	85°19′04″	85°19′31″	85°19′30″	85°19′22″	86°14′06″	86°14′28″	86°15′09″	86°15′09″	86°17′29″	86°17′29″
Major oxides (wt%)											
SiO_2	48.54	49.24	47.32	47.90	49.19	48.65	47.73	48.61	48.70	47.20	48.62
TiO_2	2.72	2.89	2.96	2.73	3.01	2.71	3.01	2.80	2.78	2.82	2.86
Al_2O_3	12.93	13.74	12.15	12.9	13.16	13.11	12.80	12.63	12.49	12.20	12.75
Fe_2O_3	16.04	16.16	16.83	16.09	16.29	16.19	16.89	17.17	15.9	16.79	17.02
MnO	0.22	0.22	0.23	0.22	0.23	0.23	0.22	0.22	0.25	0.22	0.22
MgO	5.66	4.83	4.75	4.88	4.84	5.30	5.59	5.31	5.47	4.95	5.02

(*continued on next page*)

Table 2 (*continued*)

GPS Data ↓	1	2	3	4	5	6	7	8	9	10	11
	JH5/18	JH5/19	JH6/14	JH6/15	JH6/17	JH6/18	JH6/21	JH6/23	JH6/25	JH6/35	JH8/4
Latitude	23°45′29″	23°45′55″	23°46′57″	23°47′07″	23°47′07″	23°45′04″	23°45′09″	23°44′55″	23°44′50″	23°44′24″	23°44′54″
Longitude	86°11′02″	86°11′12″	86°14′21″	86°14′44″	86°14′28″	86°11′20″	86°11′40″	86°11′05″	86°11′37″	86°11′18″	86°10′35″
CaO	10.11	9.76	9.40	9.87	9.55	9.78	10.04	9.50	9.57	9.41	9.48
Na_2O	2.16	2.36	2.23	2.30	2.30	2.30	2.18	2.21	2.22	2.14	2.30
K_2O	0.45	0.58	0.57	0.52	0.61	0.56	0.49	0.61	0.55	0.45	0.59
P_2O_5	0.28	0.31	0.34	0.32	0.33	0.29	0.24	0.30	0.30	0.28	0.30
LOI	0.94	0.69	0.76	0.80	1.10	1.14	1.27	0.32	0.12	0.48	0.33
Total	100.05	100.78	97.54	98.53	100.61	100.26	100.46	99.68	98.35	96.94	99.49
Mg#	45.20	41.13	39.75	41.49	40.99	43.35	43.62	41.96	44.43	40.80	40.81
TAS Class[na]	SAB	SAB	SAB	SAB	SAB	SAB	SAB	SAB	SAB	SAB	SAB
CIPW norm											
Q	2.76	3.29	3.28	2.66	4.05	2.53	1.62	2.85	3.55	3.50	3.02
Or	2.72	3.48	3.53	3.19	3.68	3.89	2.96	3.68	3.35	2.80	3.57
Ab	18.70	20.23	19.79	20.18	19.83	19.91	18.87	19.10	19.38	19.06	19.92
An	24.82	25.51	22.50	24.45	24.23	24.35	24.24	23.23	21.20	23.52	23.25
Di	20.48	17.96	20.17	20.18	18.26	19.48	20.91	19.14	19.77	19.81	19.14
Hy	20.95	19.63	20.11	19.51	19.67	20.75	21.17	21.9	20.96	21.09	20.99
Mt	3.63	3.62	3.90	3.69	3.67	3.66	3.82	3.88	3.65	3.91	3.85
Il	5.29	5.57	5.90	5.37	5.82	5.26	5.84	5.43	5.44	5.64	5.56
Ap	0.66	0.73	0.83	0.77	0.78	0.69	0.57	0.71	0.72	0.68	0.71
Trace elements (ppm)											
Cr	100	80	60	80	80	90	90	80	90	80	70
Ni	20	70	80	50	20	100	110	90	60	90	90
Rb	13	14	16	14	16	14	14	15	14	17	15
Ba	132	173	206	159	185	415	633	399	539	621	166
Sr	200	214	189	203	207	200	192	212	193	232	202
Nb	11	13	12	12	12	11	10	11	11	12	12
Ta	0.9	1.0	1.0	0.9	1.0	0.9	0.8	0.9	0.9	0.9	0.9
Zr	148	159	152	141	163	122	91	157	156	141	144
Hf	4.2	4.8	4.2	4.3	4.5	4.1	3.4	5.1	4.8	4.8	5.0
Y	35	38	39	37	41	36	30	39	38	37	39
Ga	23	24	21	23	27	23	24	22	21	22	23
Th	1.8	1.8	1.8	1.6	2.0	1.7	1.4	2.0	1.8	1.7	1.8
U	0.4	0.4	0.4	0.4	0.5	0.4	0.3	0.5	0.5	0.5	0.5
La	14.50	17.70	15.60	13.90	16.50	14.60	12.70	17.00	16.50	15.20	16.00
Ce	34.40	41.40	37.60	33.70	38.70	35.50	30.60	38.70	37.60	34.80	37.00
Pr	4.20	5.86	5.39	4.93	4.78	5.07	4.40	5.81	5.45	5.31	5.62
Nd	19.80	24.70	23.50	21.60	22.20	22.60	19.30	24.10	23.20	21.90	23.80
Sm	5.80	6.50	6.30	5.70	6.50	6.00	5.20	6.40	6.40	6.30	6.60
Eu	1.93	2.16	2.08	1.96	2.09	1.99	1.84	2.19	2.09	2.11	2.20
Gd	6.40	7.70	7.30	6.40	7.10	7.20	6.30	6.90	7.10	6.80	7.10
Tb	1.10	1.20	1.20	1.10	1.20	1.10	1.00	1.30	1.30	1.30	1.30
Dy	6.50	7.20	7.10	6.70	7.20	6.70	6.10	7.20	7.00	6.90	7.30
Ho	1.30	1.50	1.50	1.40	1.50	1.40	1.30	1.50	1.40	1.40	1.60
Er	3.90	4.60	4.40	4.00	4.30	4.20	3.80	4.40	4.30	4.40	4.50
Tm	0.56	0.66	0.64	0.57	0.62	0.57	0.54	0.63	0.65	0.58	0.61
Yb	3.30	3.80	3.70	3.40	3.70	3.50	3.20	3.80	3.60	3.70	3.90
Lu	0.47	0.53	0.54	0.49	0.54	0.50	0.47	0.52	0.51	0.52	0.55
Nb/La	0.76	0.73	0.77	0.86	0.73	0.75	0.79	0.65	0.67	0.79	0.75
Nb/Ce	0.32	0.31	0.32	0.36	0.31	0.31	0.33	0.28	0.29	0.34	0.32
La^N/Lu^N	3.20	3.47	3.00	2.94	3.17	3.03	2.80	3.39	3.56	3.03	3.02
La^N/Sm^N	1.57	1.71	1.56	1.54	1.60	1.53	1.54	1.67	1.62	1.52	1.53

(–) Not determined.
[a] Classification by SINCLAS computer programme (cf. Verma et al., 2002): SAB: Sub-alkaline basalt.

against their MgO contents are tested in Fig. 5C. Again both the dolerite dyke groups show distinct variations in HFSEs contents; the HTD dyke samples have higher concentrations of HFSEs than the LTD dyke samples with overlapping MgO concentrations. This suggests that both the groups are not co-genetic and possibly derived from different mantle sources. However, it is pertinent to mention here that samples from each set obey, amongst themselves, crystallization trends and which clearly suggest their co-genetic nature. As Zr is thought to be a good element to monitor differentiation, in order to reconfirm the above inferences another variation diagram deploying Zr and a few other HFSEs has been plotted (Fig. 6). In all such the plots the HTD shows higher concentrations of HFSEs than those from Ltd. All these variation plots corroborate very distinct geochemical nature for the HTD and the LTD and suggest their derivation either from distinct mantle sources or from different degrees of melting of the same source.

Fig. 7 presents primitive mantle-normalized multi-element (ME) spidergrams and chondrite- normalized rare-earth element (REE) patterns for the studied mafic dyke samples. All the plotted samples show enriched concentrations in comparison to primordial mantle and chondrite. In the first instance, it is observed that both the HTD and LTD types display different multi-elements and REE patterns corroborating geochemical features observed from the variation diagrams. A very limited variation is observed on ME and REE patterns within both the groups, however there are a number of features which clearly distinguish them. The HTD

Table 3
Whole rock major oxides (wt%), CIPW Normative compositions and trace elements (ppm) of a Cretaceous Salma dyke from the Raniganj area, Chhotanagpur gneissic terrain, Singhbhum craton, eastern India.

GPS Data ↓	1	2	3	4	5	6	7	8	9	10
	RG9/09	RG9/SM1	RG9/SM3	RG9/SM5	RG9/SM8	RG9/SM10	RG9/SM11	RG9/SM12	RG9/SM14	RG9/SM16
Latitude	23°35′39″	23°39′48″	23°37′36″	23°37′49″	23°41′18″	23°43′24″	23°43′24″	23°43′38″	23°44′30″	23°46′17″
Longitude	87°02′17″	87000′26″	87001′24″	87001′20″	86059′48″	86058′57″	86058′57″	86058′52″	86058′36″	86057′01″
Major oxides (wt%)										
SiO_2	53.04	51.95	51.44	52.18	53.23	52.38	49.82	52.73	52.70	51.96
TiO_2	1.83	1.58	1.60	1.49	1.48	1.51	1.64	1.47	1.66	1.48
Al_2O_3	14.10	15.70	14.27	15.58	14.29	14.85	15.29	14.67	14.60	14.97
Fe_2O_3	11.70	10.91	11.45	10.74	11.28	11.18	12.22	11.08	11.60	10.71
MnO	0.17	0.15	0.17	0.16	0.16	0.15	0.08	0.15	0.16	0.16
MgO	5.47	4.94	5.72	5.24	5.79	5.9	4.18	5.93	6.06	5.98
CaO	9.67	9.93	9.90	9.99	9.71	9.96	6.72	9.59	9.51	10.70
Na_2O	2.81	3.17	2.91	3.11	2.79	2.60	2.82	2.69	2.68	2.71
K_2O	0.64	0.63	0.58	0.57	0.69	0.63	0.59	0.83	0.59	0.45
P_2O_5	0.22	0.19	0.19	0.18	0.18	0.18	0.20	0.19	0.20	0.18
LOI	1.09	1.25	1.01	0.97	1.01	1.20	6.50	1.31	1.01	1.50
Total	100.74	100.40	99.24	100.21	100.61	100.54	100.06	100.64	100.77	100.80
Mg#	54.05	53.25	55.69	55.10	56.36	57.41	46.25	57.38	56.79	58.41
TAS Class[na]	BA	BA	BA	BA	BA	BA	BA	BA	BA	BA
CIPW norm										
Q	6.18	3.10	3.50	3.38	5.57	5.03	7.58	4.93	5.52	3.99
Or	3.83	3.79	3.52	3.42	4.13	3.78	3.76	4.98	3.53	2.70
Ab	24.08	27.29	25.30	26.75	23.91	22.32	25.77	23.12	22.94	23.30
An	24.28	27.21	24.82	27.31	24.75	27.39	29.50	25.90	26.37	27.78
Di	18.75	17.79	19.96	17.93	18.72	17.62	4.22	17.30	16.39	20.36
Hy	15.19	13.91	15.70	14.50	16.12	17.04	21.23	17.02	17.98	15.24
Mt	3.65	3.42	3.63	3.36	3.52	3.50	4.07	3.47	3.62	3.35
Il	3.52	3.04	3.12	2.87	2.85	2.90	3.37	2.84	3.19	2.85
Ap	0.52	0.45	0.45	0.42	0.42	0.42	0.50	0.45	0.47	0.42
Trace elements (ppm)										
Cr	160	170	220	210	190	220	190	220	190	230
Ni	40	30	40	40	30	40	30	30	30	30
Rb	10	10	9	9	14	11	10	17	10	7
Ba	212	131	140	129	556	266	211	420	376	126
Sr	315	343	303	326	278	313	312	310	279	280
Nb	8	7	9	8	7	7	9	6	7	7
Ta	0.4	0.4	0.4	0.4	0.4	0.4	0.4	0.4	0.4	0.3
Zr	106	98	96	93	93	97	106	96	95	89
Hf	3.2	2.9	2.8	2.8	2.7	2.8	3.1	2.9	2.8	2.5
Y	30	26	25	25	26	24	25	25	26	25
Ga	19	18	18	18	18	18	18	18	18	17
Th	1.2	0.9	0.9	0.9	1.1	0.9	1.2	0.8	1.1	0.8
U	0.2	0.2	0.2	0.2	0.2	0.2	0.2	0.2	0.2	0.2
La	10.30	8.80	8.70	8.30	8.60	8.40	9.40	8.40	8.70	7.70
Ce	24.30	20.80	20.60	19.90	20.10	19.70	22.20	20.50	20.50	18.00
Pr	3.10	2.67	2.66	2.56	2.57	2.55	2.81	2.69	2.60	2.35
Nd	14.60	13.10	12.80	12.40	12.60	12.50	13.10	13.00	12.40	11.50
Sm	4.40	3.90	3.90	3.70	3.80	3.80	3.90	4.10	3.90	3.50
Eu	1.52	1.39	1.34	1.33	1.35	1.31	1.36	1.51	1.38	1.26
Gd	5.40	4.60	4.70	4.50	4.60	4.50	4.50	4.80	4.70	4.20
Tb	0.90	0.80	0.80	0.80	0.80	0.80	0.80	0.80	0.80	0.70
Dy	5.40	4.50	4.70	4.50	4.70	4.50	4.60	4.90	4.70	4.20
Ho	1.00	0.90	0.90	0.90	0.90	0.90	0.90	0.90	0.90	0.80
Er	2.90	2.50	2.50	2.40	2.60	2.50	2.50	2.60	2.60	2.40
Tm	0.42	0.36	0.37	0.35	0.38	0.36	0.36	0.39	0.38	0.34
Yb	2.70	2.30	2.40	2.30	2.40	2.30	2.30	2.50	2.50	2.20
Lu	0.43	0.36	0.36	0.35	0.38	0.36	0.36	0.38	0.38	0.34
Nb/La	0.78	0.80	1.03	0.96	0.81	0.83	0.96	0.71	0.80	0.91
Nb/Ce	0.33	0.34	0.44	0.40	0.35	0.36	0.41	0.29	0.34	0.39
La^N/Lu^N	2.49	2.54	2.51	2.46	2.35	2.42	2.71	2.29	2.38	2.35
La^N/Sm^N	1.47	1.42	1.40	1.41	1.42	1.39	1.52	1.29	1.46	1.38

[a] Classification by SINCLAS computer programme (cf. Verma et al 2002): BA: Basaltic andesite.

samples lack a negative Ta anomaly but display a very minor negative Nb anomaly. On the other hand, the LTD samples show minor negative anomalies at Nb as well as Ta. With the exception of a couple of samples from the HTD group, rest of the samples from both the groups lack any negative spikes at Zr or Hf. Sr has opposite behaviour, with the HTD showing a negative anomaly, whereas the LTD has a positive spike. LTD samples also display a prominent positive anomaly at K. Positive K spikes are also reported from the Salma dyke samples (Paul, 2005) and have been attributed to late hydrothermal alteration as saussuritization in plagioclase grains is observed in many samples. The HTD samples have relatively higher REE abundances than the LTD samples and show inclined REE patterns; La^N/Lu^N ratios vary between 2.8 and 4.5 with an average of 3.1. Although, in general, REE patterns of the LTD samples are also inclined (La^N/Lu^N ratios vary between 2.3 and 2.5), however, they are slightly different than those of the

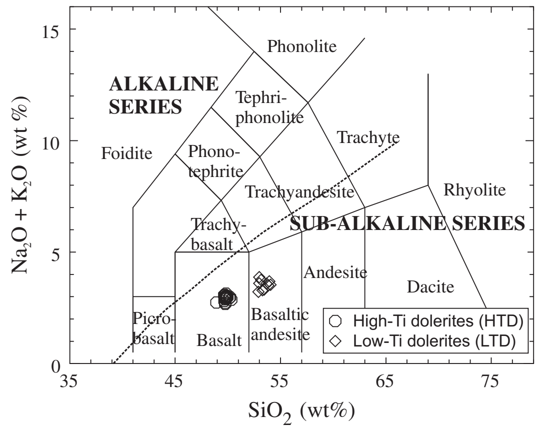

Fig. 4. Total-alkali silica (TAS) classification diagram (after Le Maitre, 2002); dotted line discriminates between sub-alkaline basalts and alkaline basalts (after Irvine and Baragar, 1971).

HTD samples; likewise, middle REE (MREE) abundances in LTD are relatively slightly higher and also have flat heavy REE (HREE) patterns.

Now before any further evaluation of geochemistry of the studied mafic dykes it would be better to discuss possible role of crustal contamination during their emplacement first. Many workers suggested that possibility of crustal contamination in dykes, particularly in their homogeneous central parts, is negligible as compared to volcanic rocks (Gill and Bridgwater, 1979; Kalsbeek and Taylor, 1986; Tarney and Weaver, 1987; Radhakrishna et al., 1991; Srivastava and Singh, 2004; Srivastava et al., 2009). During the present study most of the studied dyke samples were collected from the homogeneous centre part of dykes to minimize any possible contamination. However, possibility of some degree of contamination in mantle derived magmas during their ascent and/or temporary residence in crustal magma chambers cannot be absolutely discarded (Mohr, 1987). Although it is difficult to assess crustal contamination without having isotope data, some critical geochemical characters may help to identify possible involvement of crustal material during emplacement of mafic magmas. Ti/Y and Ba/Nb ratios of present studied mafic dyke samples are compared with mantle derivatives (MORB, OIB and Primordial Mantle) and average crust values (Fig. 8) and it can be seen that most of the studied samples plot closer to mantle derivatives. However, a few samples show their tendency towards average crust. This probably indicates that

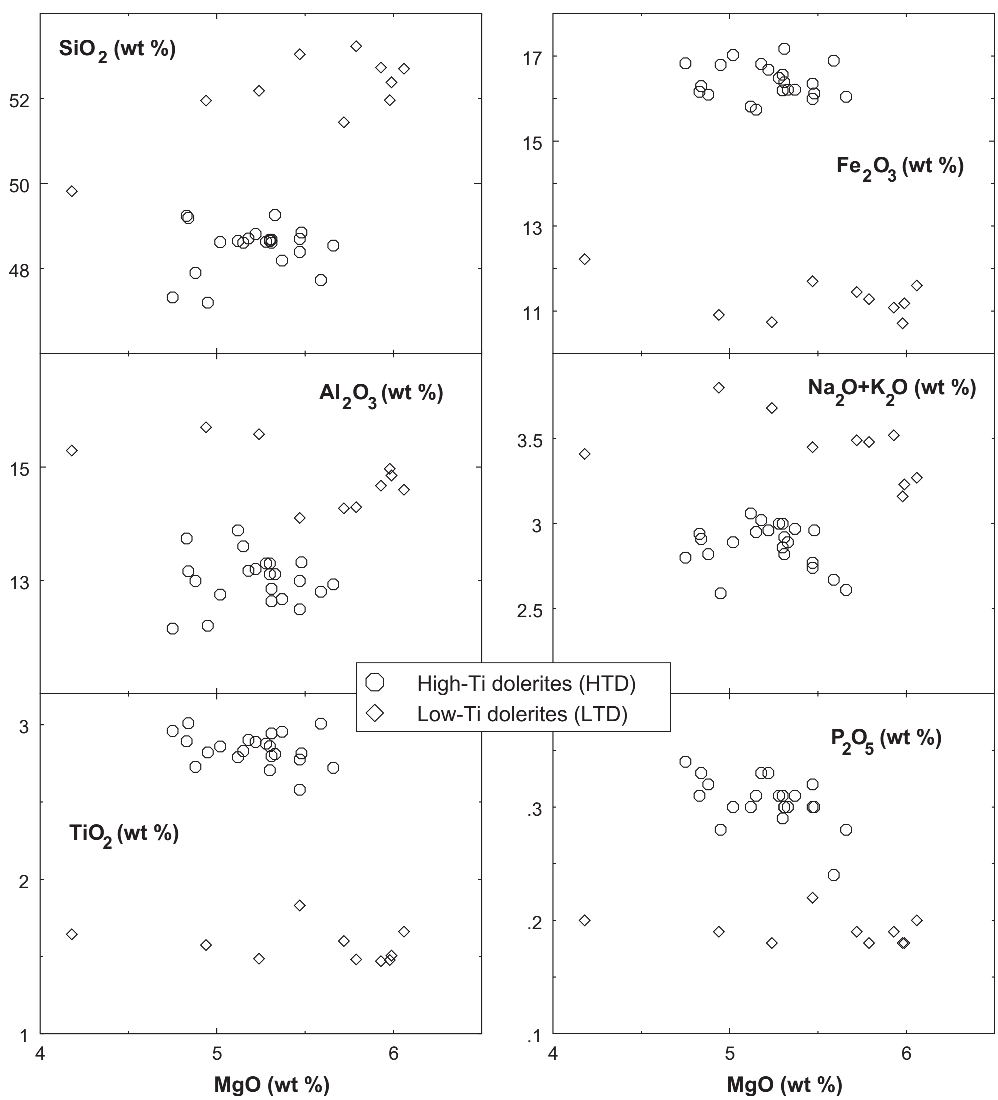

Fig. 5A. Harker-type variation diagram for major oxides against MgO.

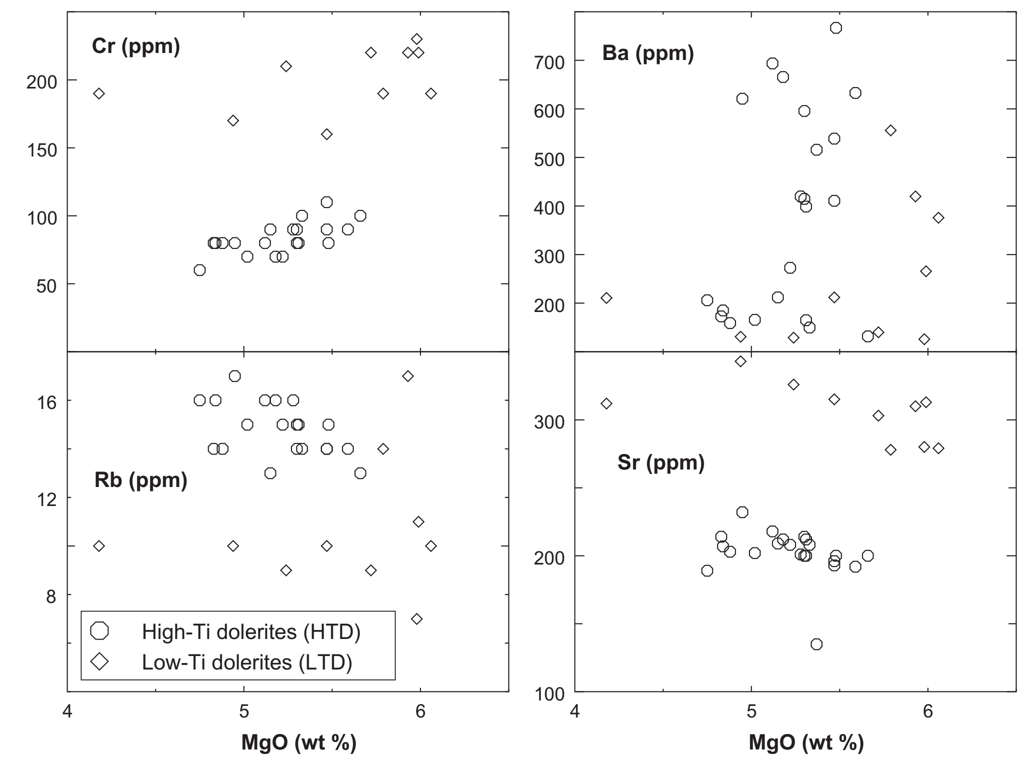

Fig. 5B. Harker-type variation diagram for Cr and LILEs against MgO.

the lower crust may have little influence in the petrogenesis of the studied dykes. Further, Nb/La, Nb/Ce, and La^N/Sm^N ratios of studied mafic dykes are also compared with primordial mantle and average crust values (see Table 4). These ratios are more close to the primordial mantle values than the average crust which also discourages any serious role of crustal contamination in genesis of the studied mafic dykes.

Behaviour of Nb–Ta, Hf–Zr, Sr and REE patterns have also been successfully used to identify the involvement of crustal contamination as well as subduction processes. Crustally contaminated samples are expected to show significant negative Nb (Ta) and Zr (Hf) and positive Sr anomalies on ME spidergrams (Crawford, 1989; Tatsumi and Eggins, 1995; Srivastava and Singh, 2004; Zhao and Zhou, 2007; Cai et al., 2010; Srivastava et al., 2012). Besides, the crustally contaminated samples or addition of subducted component to mantle melt should also display LREE enrichment patterns. The HTD samples clearly do not show these geochemical features on the ME and REE plots which precludes any significant crustal contamination in these dykes. Although, the LTD samples have some geochemical features which indicate possibility of crustal contamination, absence of negative Zr (Hf) anomaly and inclined REE patterns in these samples (see Fig. 7) exclude significant crustal contamination. Further, La^N/Sm^N ratios are relatively very low (see Tables 2 and 3), the average being 1.57 in the HTD and 1.42 in the LTD, in the studied mafic dykes in comparison to average crust which has La^N/Sm^N ratio ~4.30 (see Table 4). Additionally, Zr/Y, Nb/Y (Fig. 9) and Th/Ta, La/Ta (Fig. 11B) ratios, discussed later in "Discussion section", also preclude any serious crustal contamination in the studied rocks. Therefore, on the basis of the available geochemical data it may be suggested that the composition of the studied mafic dykes were not significantly affected by crustal contamination, and isotopic data is needed to confirm this inference. Nevertheless, geochemical data of the present study may be utilized to discuss geochemical behavior and petrogenesis of the studied mafic dykes.

Nature of the REE patterns may also be used to understand degree of melting conditions (Cullers and Graf, 1984). Hirschmann et al. (1998) stated that in many cases low percentage melting of a mantle source may produce slightly fractionated REE patterns, whereas flat REE patterns are produced by higher percentage of mantle melting. Although samples of both sets of mafic dykes show inclined REE patterns, the slope of the HTD samples is relatively steeper than that of the LTD samples; La^N/Lu^N ratios is higher in the HTD samples than those in the LTD samples (see Tables 2 and 3). Therefore, on the basis of observed REE patterns, it may be suggested that the HTD samples are crystallized from a relatively low percentage of melting of a mantle source than the LTD samples, which probably derived from a rather higher percentage of melting (cf. Hirschmann et al., 1998).

6. Discussion

The petrographic and geochemical characteristics of the studied Cretaceous mafic dykes emplaced within the Gondwana sedimentary basins of the Damodar valley and its environs permit us to classify them into two distinct magmatic types. One set of mafic dykes trending in NNE to ENE directions shows comparatively higher concentrations of titanium, iron and HFSEs than the other set of mafic dykes, which trend in NW to NNW direction. The dykes with high titanium are identified as high-Ti dolerite (HTD) dykes, whereas the dykes with comparatively low titanium are recognized as low-Ti dolerite (LTD) dykes. Both these distinct mafic dykes appear to be genetically unrelated. As temporal aspects of mafic dykes play an important role in understanding their petrogenesis, it is important to discuss the available geochronological and paleomagnetic information on them. One of the mafic dykes from the study area, the Salma dyke, has been dated by Ar–Ar method to be of 65.1 ± 0.3 Ma (Kent et al., 2002) which is close to the Deccan event, whereas majority of the other mafic dykes have ages between 110

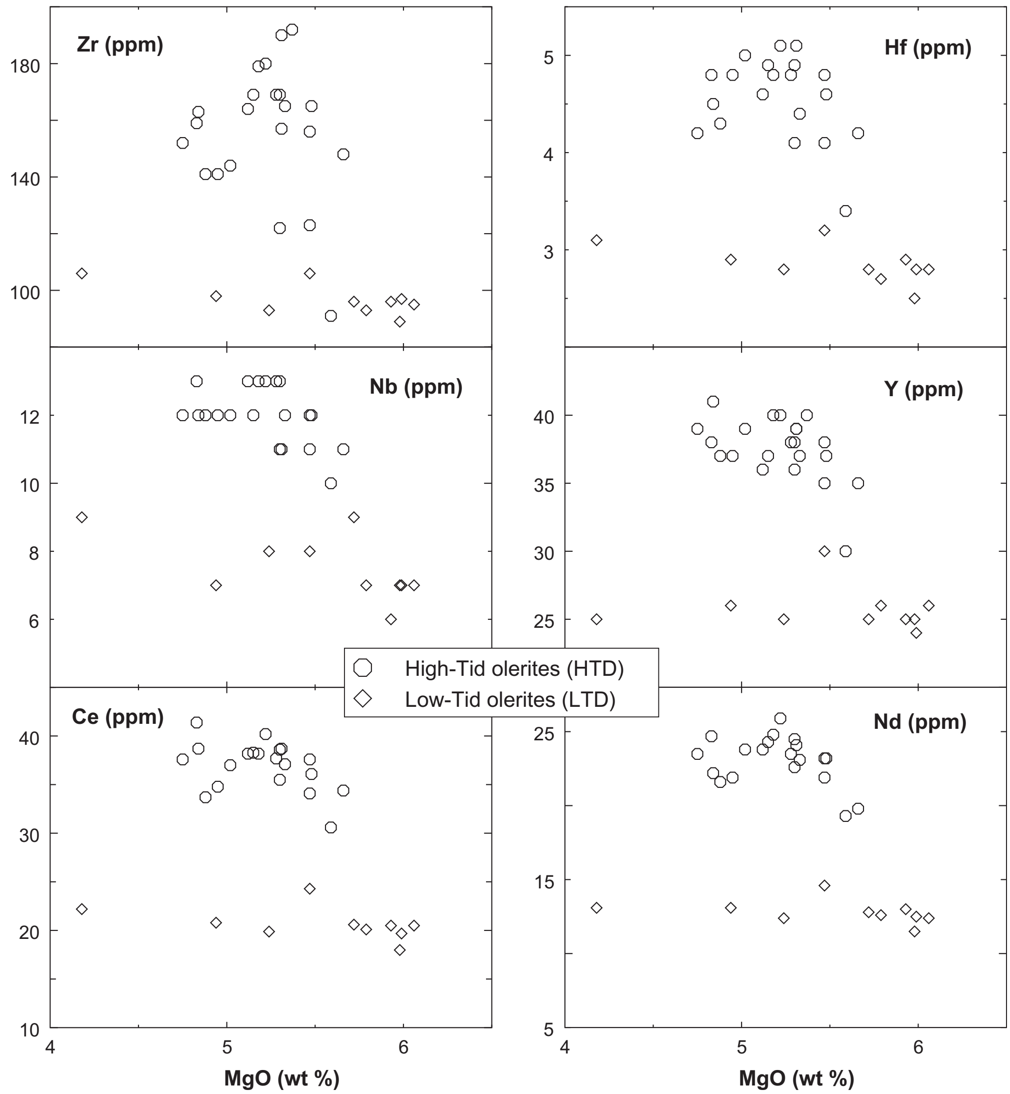

Fig. 5C. Harker-type variation diagram for HFSEs against MgO.

and 115 Ma (Agarwal and Rama, 1976; Kent et al., 1997, 2002), and have been linked to Kerguelen plume activity (Coffin et al., 2002; Kent et al., 2002; Srivastava and Sinha, 2007). All the available ages on Cretaceous mafic dykes and Rajmahal basalts of the CGT and Damodar valley sedimentary basins are presented in Table 1.

From the Table 1 it is observed that Rajmahal and Bengal basin tholeiitic basalts are erupted during 118–116 Ma, whereas ages of most mafic dykes were slightly younger and emplaced between 110 and 115 Ma. Kent et al. (2002) also recorded a number of younger ages, between 109 Ma and 102 Ma, for Rajmahal basalts but regarded them to be less reliable. However, the Salma dyke emplaced at ~65 Ma is an exception to these ages and it is interesting to note that this dyke is spatially close to the Rajmahal Traps rather than the Deccan Traps (Kent et al., 2002; Paul, 2005), and its palaeomagnetic pole at ~117 Ma (Patil and Arora, 2008), is close to the age of the Rajmahal basaltic eruptions. Paul (2005) has studied samples of the Salma dyke for their geochemical characteristics and found some interesting results; trace element (mainly HFSEs) composition of the Salma dyke samples is similar to those of the Rajmahal Group I basalts (Storey et al., 1992; Kent et al., 1997), whereas REE contents are close to those of the Deccan mafic dykes (Mahoney et al., 2000). It is important to mention here that a dolerite dyke emplaced just adjacent to the Salma dyke at Kalidaspur, Raniganj basin, having same trend as the Salma dyke, gave an Ar–Ar age 112.5 ± 0.5 Ma (Kent et al., 2002). Additionally, one of the mafic dykes trending in similar direction (i.e. NW) and exposed near Koderma has been dated at 115.3 ± 0.4 Ma (Kent et al., 2002). In the present study, a sample of the Kalidaspur dyke (RG9/09), which is exposed adjacent to the Salma dyke, is also analysed and its geochemistry (both trace and rare-earth elements) is very similar to that of the Salma dyke samples (see Table 3). It is indeed surprising to have two dykes sharing similar chemistry, petrography and field setting yielding two different emplacement ages at ~65 Ma and ~112–115 Ma. A re-look at the geochronological and paleomagnetic aspects of the Salma as well as the other dykes is mandatory to resolve this issue. The following sections would attempt to seek answer to the pertinent questions such as – (i) whether the studied mafic dykes are mantle plume-derived melts? (ii) if yes, whether they are related to the Kerguelen mantle plume or to the Rèunion mantle plume? and (iii) whether all the NW to NNW trending dykes, including Koderma and the Salma, are co-genetic and co-eval?

In the Zr/Y and Nb/Y plot (Fig. 9), which is widely used to identify plume-derived melts signature (Fitton et al., 1997; Baksi,

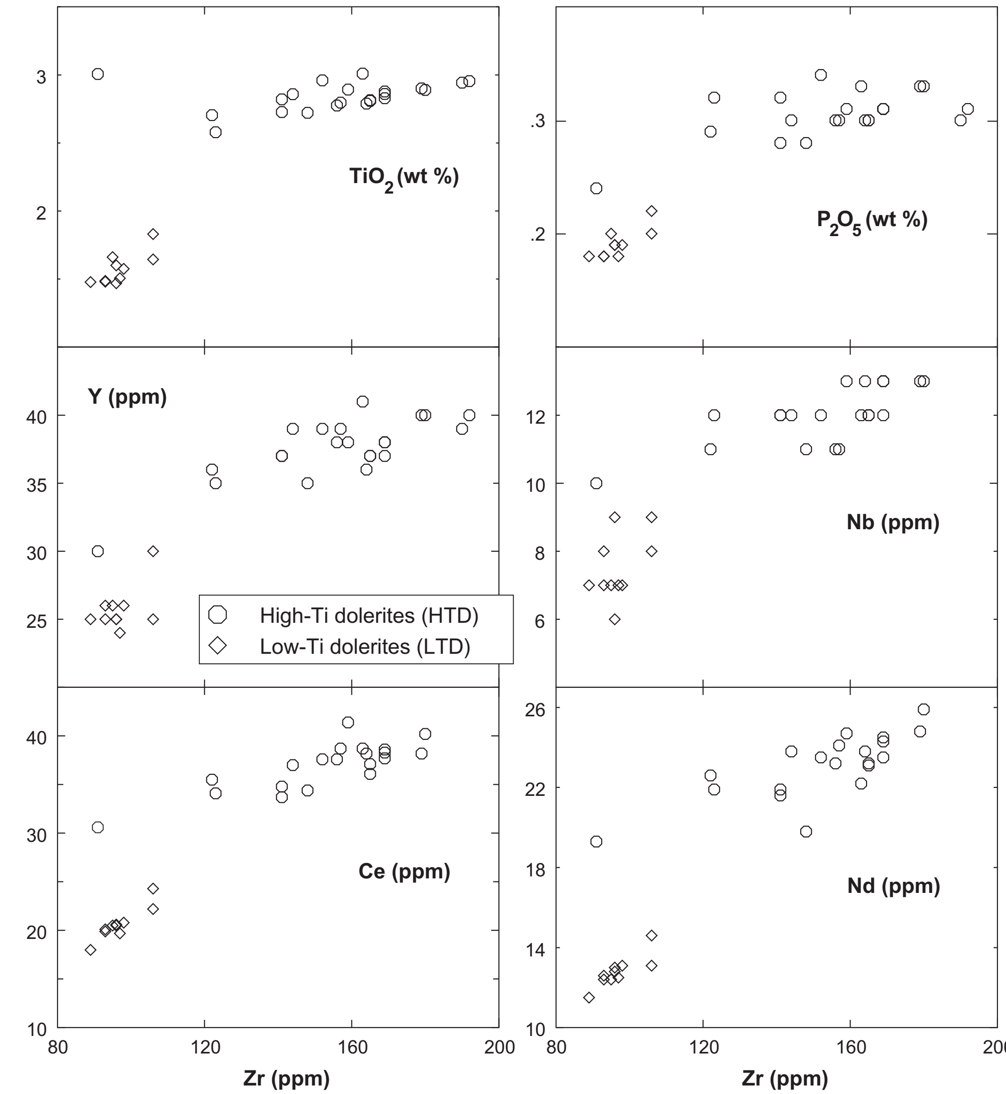

Fig. 6. Zr vs HFSEs variation plots.

2000), all the studied samples plot within the plume-derived basalt field. This demonstrates their linkage to plume activity and it becomes pertinent to evaluate the relative melt contribution of the Kerguelen and Rèunion mantle plumes in their genesis. A comparison of geochemical data of the mafic dykes from the CGT and Damodar valley with that of the Rajmahal basalts by previous workers (Kent et al., 1997; Paul, 2005) is contradictory in nature. For example, Kent et al. (1997) have presented geochemical data for the mafic dyke samples from the Koderma, Raniganj basin (which also includes one sample from the Salma dyke), and Jharia basin. They stated that geochemical data of the mafic dykes of Raniganj basin matches with that of the Rajmahal Group I basalts, whereas that of the Koderma mafic dyke samples corresponds to that of the Rajmahal Group II basalts. However, geochemical data of the Jharia basin mafic dyke and the Salma dyke do not match with any of the Rajmahal basalts but correspond to the Deccan chemistry. On the other hand, Paul (2005) points out that trace element chemistry of the Salma dyke samples show similarities with Rajmahal Group I basalts. Geochemical data of Kent et al. (1997) and geochemical data of mafic dyke samples of present study are also compared (Fig. 10) and an altogether different picture emerges; both the Koderma and Raniganj basin mafic dyke samples of Kent et al. (1997) show close geochemical similarities with the LTD samples of present study, whereas the Salma dyke and Jharia basin samples of Kent et al. (1997) match with the HTD samples. This is surprising because most of the LTD samples of present study are from the Salma dyke. This necessitates a re-look at the reported age of the Salma dyke at ~65 Ma (Kent et al., 1997) especially so as its paleomagnetic pole matches well with that of the Rajmahal Traps (Patil and Arora, 2008). It is also possible that Salma dyke may represent a composite dyke that channelised Rajmahal as well as Deccan magmas and therefore its detailed mapping is required to establish multiple intrusions, if any. However, there is no other reliable age for any mafic unit, either intrusive or extrusive (except the Salma mafic dyke sample), in this domain relating their links to the Deccan event (see Table 1).

Another important question arises as to whether chemistry alone can be an effective discriminant to distinguish the signatures of the Rajmahal and the Deccan Traps? To answer this, samples of the present study together with those of Kent et al. (1997) are compared with mafic rocks/basalts derived from Kerguelen and Rèunion plume (particularly Deccan) activities. The studied samples (both HTD and LTD) and also those samples analysed by Kent et al. (1997) show very close similarities with the samples derived from Kerguelen plateau basalts (Fig. 11). All the samples of this study also show very close geochemical resemblance to the Rajmahal Group I tholeiites and not to the Group II tholeiites (Storey et al., 1992; Kent et al., 1997). Other important observation

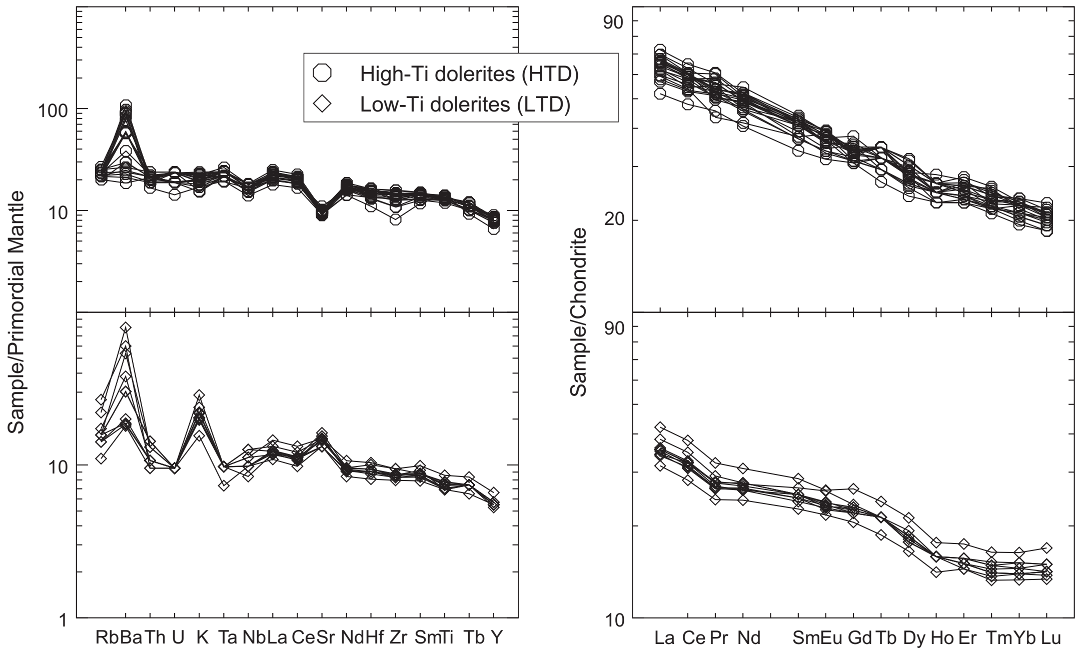

Fig. 7. Primordial mantle normalized multi-element spidergrams and chondrite normalized rare-earth element patterns for distinct Cretaceous mafic dykes from the Chhotanagpur Gneissic Terrain. Primordial mantle and chondrite values are taken from McDonough et al., 1992 and Evensen et al., 1978).

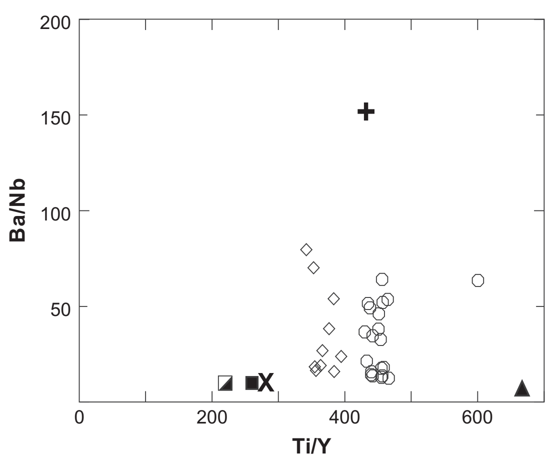

Fig. 8. Ti/Y vs. Ba/Nb ratio variation diagrams. Symbols used are: + average lower crust (Weaver and Tarney, 1984), N-MORB (half-filled square; Humphris et al., 1985), ■ E-MORB (Humphris et al., 1985), ▲ OIB (Sun, 1980), and x primordial mantle (McDonough et al., 1992).

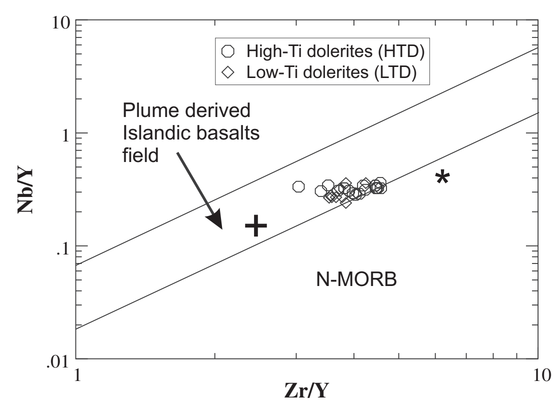

Fig. 9. Nb/Y vs. Zr/Y ratio plot for samples of present study compared with primordial mantle (PM; after McDonough and Sun, 1995), and average continental crust (AC; after Rudnick and Fountain, 1995).

from Th/Ta vs La/Ta double ratio plot (Fig. 11B) is that studied samples fall close to the Primordial Mantle value and away from that of the average crust value suggesting least or no significant involvement of crustal material in their petrogenesis. The studied mafic dyke samples together with those from Kent et al. (1997) are also compared with those from the Deccan flows and dykes (Fig. 12). All

Table 4
Nb/La, Nb/Ce, and La^N/Sm^N ratios of studied mafic dykes from the Chhotanagpur Gneissic Terrain, Singhbhum craton, eastern India, primordial mantle and average crust for comparison.

	Nb/La	Nb/Ce	La^N/Sm^N
High-Ti dolerites (HTD)	0.65–0.86 (Av. 0.77)	0.28–0.36 (Av. 0.32)	1.51–1.71 (Av. 1.57)
Low-Ti dolerites (LTD)	0.71–1.03 (Av. 0.86)	0.29–0.44 (Av. 0.36)	1.29–1.52 (Av. 1.42)
Primordial mantle	1.01	0.39	1.00
Average crust	0.46	0.23	4.30

Av.: Average value; Primordial mantle and average crust values are taken from McDonough et al. (1992) and Weaver and Tarney (1984), respectively.

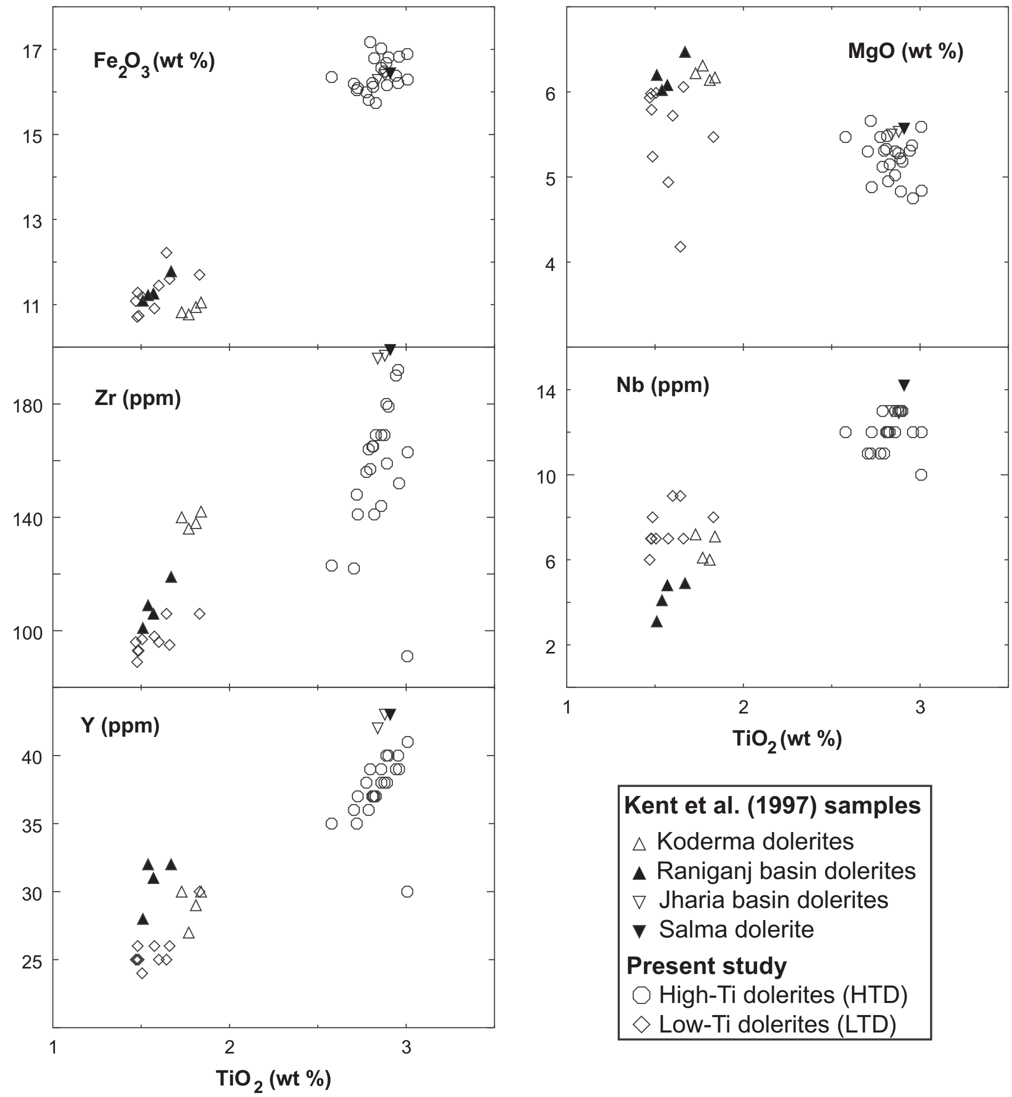

Fig. 10. TiO_2 vs Fe_2O_3, MgO and few HFSEs to compare samples of present study with Kent et al. (1997).

of them also show close similarities with Deccan basalts and dykes; the LTD samples match with low-Ti flows and dykes, whereas the HTD samples display close similarities with intermediate-Ti flows and high-Ti dykes. Thus, the studied samples from the CGT and Damodar valley show close geochemical similarities with both Kerguelen and Rèunion plume derived rocks and two broad conclusions may be inferred: – (i) all of them are derived from plume tectonics and (ii) it is difficult to assign their association to any particular plume based solely on the basis of geochemistry.

As a number of ages (118–105 Ma), that are available for different igneous rocks exposed all around the eastern and northeastern Indian shield, show their temporal similarity to the Rajmahal volcanic event (see Table 1) we prefer to link the mafic dykes of this study to the Kerguelen plume activity. It has been observed that most of the alkaline rocks (alkaline–carbonatite complexes and lamprophyres of the Shillong plateau) and mafic dykes (both from the Shillong plateau and the CGT including Damodar valley) from eastern and NE India have younger ages (between 115 Ma and 105 Ma) than that of the Rajmahal and Bengal basin basalts (117–118 Ma). In the present study it is observed that the HTD samples have higher contents of HFSEs than that of LTD and are derived from lower percentage of melting of a mantle source. As it is well-established that alkaline rocks are melts generated through lower percentage of melting, it likely that the HTD are emplaced during later stages of Kerguelen plume activities than the LTD. However, it is essential to have robust geochronological and paleomagnetic data on both sets of mafic dykes to confirm these aspects. Such a study will also address the enigmatic problem related to the Deccan-age of the Salma dyke.

7. Conclusions

A number of mafic dykes having distinct structural trends (NNE to ENE and NW to NNW) are emplaced in the Damodar valley, Chhotanagpur Gneissic Terrain, at the northern-most margin of the Singhbhum craton. A majority of them intrude the coal-bearing Gondwana sedimentary basins but a few of them also cut across the Precambrian rocks. Petrographic and geochemical characteristics of the Cretaceous mafic dykes classify them into two distinct types – high titanium dolerites and Low-titanium dolerites and

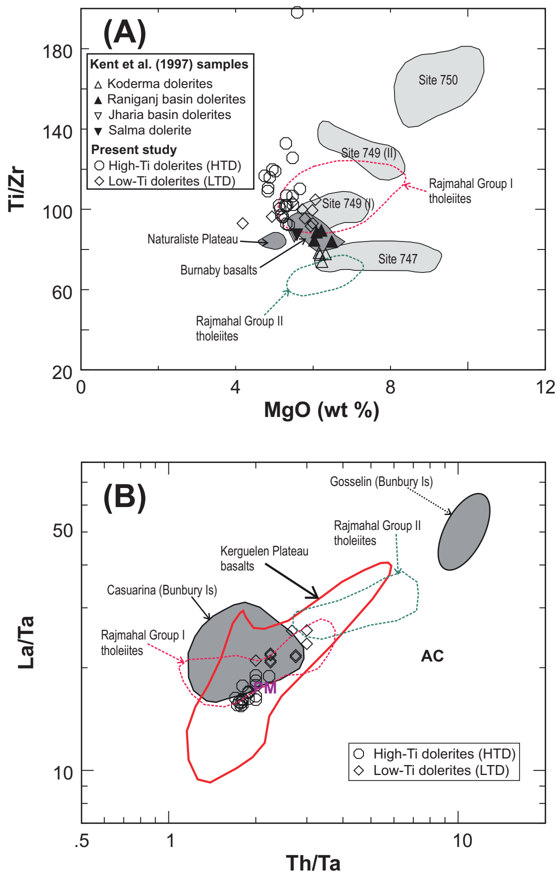

Fig. 11. Samples of present study and Kent et al. (1997) are compared with the Kerguelen plume induced magmatic rocks. (A) MgO (wt%) vs Ti/Zr ratio for Kerguelen plateau (Sites 750, 749 I and II, and 747), Naturaliste plateau, Bunbury basalt, and Rajmahal tholeiites (Fields are after Storey et al., 1992); (B) Th/Ta vs Ti/Zr ratios plot for Kerguelen plateau basalts (Salters et al., 1992; Mahoney et al., 1995), Rajmahal Group I and II basalts (Storey et al., 1992), and Bunbury island (both Gosselin and Casuarina types) basalts (Frey et al., 1996). Fields are taken from Kent et al. (1997).

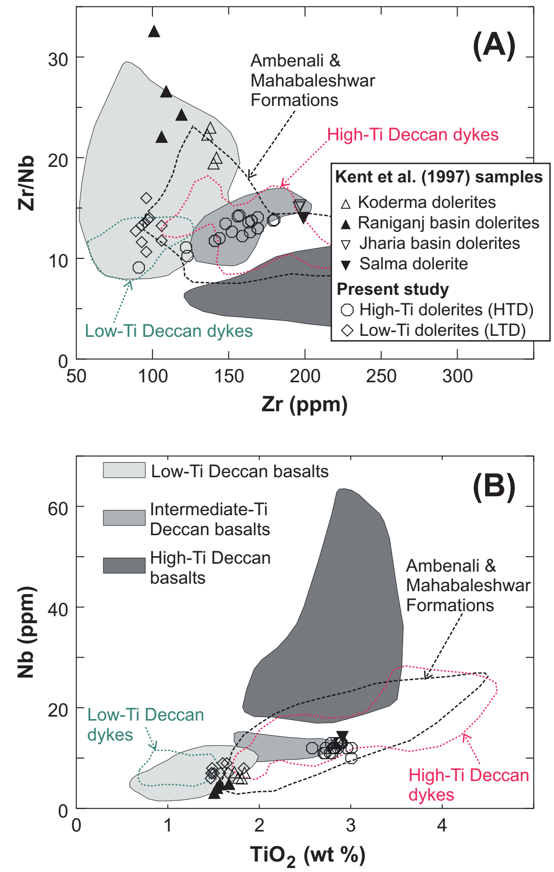

Fig. 12. (A) Zr vs Zr/Nb plot and (B) TiO_2 vs Nb plot for samples of present study and Kent et al. (1997) and compared with the Deccan volcanics and dykes. Deccan volcanic basalts fields are from Melluso et al. (1995) and Deccan mafic dykes are from Melluso et al. (1999).

bring-out their different petrogenesis. Available ages on these dykes suggest their emplacement ~110–115 Ma, however one of them viz. the Salma dyke, has been dated ~65 Ma. Even though the studied rocks show undoubted plume-derived signature it is not possible to decipher their unequivocal lineage with either the Rajmahal or the Deccan-related mafic rocks from geochemistry alone. Robust geochronological and paleomagnetic measurements on carefully selected samples are clearly required to constrain the relative contributions of the Kerguelen- and the Reunion- mantle plume activities in the genesis of Cretaceous mafic dykes from this domain.

Acknowledgements

The Department of Science and Technology, New Delhi is thankfully acknowledged for providing research Grant for the present work (ESS/16/299/2006). Authors are thankful to Ray W. Kent and an anonymous reviewer for their constructive comments on the earlier version which helped us to considerably improve the MS. Authors are grateful to the Head, Department of Geology, Banaras Hindu University for providing all necessary facilities during this work. We would also like to thank Guest editors Hetu C. Sheth and Loÿc Vanderkluysen for inviting us to contribute a paper to the special issue in Honour and Memory of John J. Mahoney.

References

Acharyya, S.K., 2003. The nature of Mesoproterozoic central Indian Tectonic zone with exhumed and reworked older granulites. Gondwana Research 6, 197–214.
Agarwal, J.K., Rama, 1976. Chronology of Mesozoic volcanics of India. Proceedings Indian Academy of Science 84A, 157–179.
Athavale, R.N., Verma, R.K., 1970. Palaeomagnetic results on Gondwana dykes from the Damodar valley coal fields and their bearing on the sequence of Mesozoic igneous activity in India, Geophysical. Journal Royal Astronomical Society London 20, 303–316.
Baer, G., Heimann, A., 1995. Physics and Chemistry of Dykes. Balkema, Rotterdam.
Baksi, A.K., 1995. Petrogenesis and timing of volcanism in the Rajmahal flood basalt province, northeastern India. Chemical Geology 121, 73–90.
Baksi, A.K., 2000. Search for a deep-mantle component in mafic lavas using Nb–Y–Zr plot. Canadian Journal of Earth Sciences 38, 813–824.
Bhattacharya, D.K., Mukherjee, D., Barla, V.C., 2010. Komatiite within Chhotanagpur Gneissic Complex at Semra, Palamau district, Jharkhand: Petrological and geochemical fingerprints. Journal of the Geological Society of India 76, 589–606.
Bleeker, W., 2004. Taking the pulse of planet Earth: a proposal for a new multidisciplinary flagship project in Canadian solid Earth sciences. Geoscience Canada 31, 179–190.
Bleeker, W., Ernst, R.E., 2006. Short-lived mantle generated magmatic events and their dyke swarms: the key unlocking Earth's paleogeographic record back to 2.6 Ga. In: Hanski, E., Mertanen, S., Rämö, T., Vuollo, J. (Eds.), Dyke Swarms – Time Markers of Crustal Evolution, Taylor & Francis, London, pp. 3–26.
Bryan, S.E., Ernst, R.E., 2008. Revised definition of large igneous provinces (LIPs). Earth Science Reviews 86, 175–202.
Cai, K., Sun, M., Yuan, C., Zhao, G., Xiao, W., Long, X., Wu, F., 2010. Geochronological and geochemical study of mafic dykes from the northwest Chinese Altai: implications for petrogenesis and tectonic evolution. Gondwana Research 18, 638–652.
Chalapathi Rao, N.V., Lehmann, B., 2011. Kimberlites, flood basalts and Mantle plumes: new insights from the Deccan large igneous province. Earth-Science Reviews 107, 315–324.
Chalapathi Rao, N.V., Burgess, R., Lehmann, B., Mainkar, D., Pande, S.K., Hari, K.R., Bodhankar, N., 2011. $^{40}Ar/^{39}Ar$ ages of mafic dykes from the Mesoproterozoic

Chhattisgarh basin, Bastar craton, Central India: implication for the origin and spatial extent of the Deccan large igneous province. Lithos 125, 994–1005.
Chenet, A.L., Quidelleur, X., Fluteau, F., Courtillot, V., 2007. 40K–39Ar dating of the main Deccan large igneous province: further evidence of KTB age and short duration. Earth and Planetary Science Letters 263, 1–15.
Coffin, M.F., Eldholm, O., 2005. Large igneous provinces. In: Selley, R.C., Cocks, R., Plimer, I.R. (Eds.), Encyclopedia of Geology. Elsevier, Oxford, pp. 315–323.
Coffin, M.F., Pringle, M.S., Duncan, R.A., Gladezenko, T.P., Storey, M., Mqller, R.D., Gahagan, L.A., 2002. Kerguelen hotspot magma output since 130 Ma. Journal of Petrology 43, 1121–1139.
Courtillot, V., Féraud, G., Maluski, H., Vandamme, D., Moreau, M.G., Besse, J., 1988. Deccan flood basalts and the Cretaceous/tertiary boundary. Nature 333, 843–846.
Crawford, A.J., 1989. Boninites and Related Rocks. Unwin Hyman, London.
Cullers, R.L., Graf, J.L., 1984. Rare earth elements in igneous rocks of the continental crust: predominantly basic and ultrabasic rocks. In: Henderson, P. (Ed.), Rare Earth Element Geochemistry. Elsevier, Amsterdam, pp. 237–274.
Devaraju, T.C., 1995. Dyke swarms of Peninsular India. Memoir 33. Geological Society of India, Bangalore.
Ernst, R.E., Buchan, K.L., 1997. Giant radiating dyke swarms: their use in identifying pre-Mesozoic large igneous provinces and mantle plumes. In: Large Igneous Provinces: Continental, Oceanic, and Planetary Volcanism, Mahoney, J., Coffin, M. (Eds.), Geophysical Monograph Series, vol. 100. American Geophysical Union, pp. 297–333.
Ernst, R.E., Buchan, K.L., 2001. The use of mafic dyke swarms in identifying and locating mantle plumes. In: Ernst, R.E., Buchan, K.L. (Eds.), Mantle Plumes: Their Identification Through Time. Geological Society of America Special Paper 352, pp. 247–265.
Ernst, R.E., Srivastava, R.K., Bleeker, W., Hamilton, M., 2010. Precambrian Large Igneous Provinces (LIPs) and their dyke swarms: new insights from high-precision geochronology integrated with paleomagnetism and geochemistry. Precambrian Ressearch 183, vi–xi.
Evensen, N.M., Hamilton, P.J., O'Nion, R.K., 1978. Rare earth abundances in chondritic meteorites. Geochimica et Cosmochimica Acta 42, 1199–1212.
Fahrig, W.F., 1987. The tectonic setting of continental mafic dyke swarms: failed arm and early passive margin. In: Halls, H.C., Fahrig, W.F. (Eds.), Mafic Dyke Swarms. Geological Association of Canada Special Paper 34, pp. 331–348.
Fitton, J.G., Saunders, A.D., Norry, M.J., Hardarson, B.S., Taylor, R.N., 1997. Thermal and chemical structure of the Iceland plume. Earth and Planetary Science Letters 153, 197–208.
Floyd, P.A., Winchester, J.A., 1978. Identification and discrimination of altered and metamorphosed volcanic rocks using immobile elements. Chemical Geology 21, 291–306.
Foulger, G.R., 2010. Plates vs plumes: a geological controversy. Wiley-Blackwell, Oxford.
Frey, F.A., McNaughton, N.J., Nelson, D.R., deLaeter, J.R., Duncan, R.A., 1996. Petrogenesis of Bunbury basalts, western Australia: interaction between the Kerguelen plume and Gondwana lithosphere? Earth and Planetary Science Letters 141, 163–183.
Gale, G.H., Dabek, L.B., Fedikow, M.A.F., 1997. The application of rare earth element analyses in the exploration for volcanogenic massive sulfide type deposits. Exploration and Mining Geology 6, 233–252.
Ghose, N.C., 1983. Geology, tectonics and evolution of the Chhotanagpur granite gneiss complex, Eastern India. In: Sinha-Roy, S. (Ed.), Structure and Tectonics of Precambrian Rocks of India, Recent Researches in Geology 10. Hindustan Publishing Corporation, New Delhi, pp. 211–247.
Ghose, N.C., Chatterjee, N., 2008. Petrology, tectonic setting and source of dykes and related magmatic bodies in Chotanagpur gneissic complex, eastern India. In: Srivastava, R.K., Sivaji, C., Chalapathi Rao, N.V. (Eds.), Indian Dyke: Geochemistry, Geophysics and Geochronology, Narosa Publishing House Pvt Ltd, New Delhi, pp. 471–493.
Ghose, N.C., Mukherjee, D., Chatterjee, N., 2005. Plume generated Mesoproterozoic mafic–ultramafic magmatism in the Chotanagpur mobile belt of eastern Indian shield margin. Journal of the Geological Society of India 66, 725–740.
Gill, R.C.O., Bridgwater, D., 1979. Early Archaean basic magmatism in west Greenland: the geochemistry of the Ameralik dykes. Journal of Petrology 20, 695–726.
Halls, H.C., 1982. The importance and potential of mafic dyke swarms in studies of geodynamic process. Geosciences Canada 9, 145–154.
Halls, H.C., Fahrig, W.F., 1987. Mafic Dyke Swarms. Geological Association of Canada Special Paper 34.
Hanski, E., Mertanen, S., Rämö, T., Vuollo, J., 2006. Dyke Swarms: TimeMarkers of Crustal Evolution. Taylor and Francis, London.
Heaman, L.M., Srivastava, R.K., Sinha, A.K., 2002. A precise U–Pb zircon/baddeleyite age for the Jasra igneous complex, Karbi-Analong district, Assam, NE India. Current Science 82, 744–748.
Hirschmann, M.M., Ghiorso, M.S., Wasylenki, L.E., Asimow, P.D., Stolper, E.M., 1998. Calculation of peridotite partial melting from thermodynamic models of minerals and melts. I. Method and composition to experiments. Journal of Petrology 39, 1091–1115.
Humphris, S.E., Thompson, G., Schilling, J.-G., Kingsley, R.A., 1985. Petrological and geochemical variations along the Mid-Atlantic Ridge between 46°S and 32°S: influence of the Tristan da Cunha mantle plume. Geochimica et Cosmochimica Acta 49, 1445–1464.
Irvine, T.N., Baragar, W.R.A., 1971. A guide to chemical classification of the common volcanic rocks. Canadian Journal of Earth Sciences 8, 523–548.
Jochum, K.P., Verma, S.P., 1996. Extreme enrichment of Sb, Tl, and other trace elements in altered MORB. Chemical Geology 130, 289–299.
Kalsbeek, F., Taylor, P.N., 1986. Age and origin of early Proterozoic dolerite dykes in south–west Greenland. Contribution to Mineralogy and Petrology 89, 307–316.
Karkare, S.G., Srivastava, R.K., 1990. Regional dyke swarms related to the Deccan Trap Alkaline Province, India. In: Parker, A.J., Rickwood, P.C., Tucker, D.H. (Eds.), Mafic dykes and emplacement mechanism. A.A.Balkema, Rotterdam, pp. 335–347.
Kent, R.W., 1991. Lithosphere uplift in eastern Gondwana: evidence for a long lived mantle plume system? Geology 19, 19–23.
Kent, R.W., Saunders, A.D., Storey, M., Ghose, N.C., 1996. Petrology of early Cretaceous flood basalts and dykes along the rifted volcanic margin of eastern India. Journal of Southeast Asian Earth Sciences 13, 95–111.
Kent, R.W., Saunders, A.D., Kempton, P.D., Ghose, N.C., 1997. Rajmahal basalts, Eastern India: mantle sources and melt distribution at a volcanic rifted margin, large igneous provinces: continental, oceanic and planetary volcanism. Geophysical Monograph, American Geophysical Union 100, 145–182.
Kent, R.W., Kelley, S.P., Pringle, M.S., 1998. Mineralogy and 40Ar/39Ar geochronology of orangeites (Group II kimberlites) from the Damodar valley, eastern India. Mineralogical Magazine 62 (3), 313–323.
Kent, R.W., Pringle, M.S., Muller, R.D., Saunders, A.D., Ghose, N.C., 2002. 40Ar/39Ar Geochronology of the Rajmahal basalts, India and their relationship to the Kerguelen Plateau. Journal of Petrology 43, 1141–1153.
Kumar, A., Ahmad, T., 2007. Geochemistry of the mafic dykes in parts of Chotanagpur gneissic complex: petrogenetic and tectonic implications. Geochemical Journal 41, 173–186.
Le Maitre, R.W., 2002. Igneous Rocks: A Classification and Glossary of Terms. Cambridge University Press, Cambridge.
Mahadevan, T.M., 2002. Geology of Bihar and Jharkhand. Geological Society of India, Bangalore.
Mahoney, J.J., Jones, W.B., Fret, F.A., Salters, V.J.M., Pyle, D.G., Davies, H.L., 1995. Geochemical characteristics of lavas from Broken Ridge, the Naturaliste Plaleau and southernmost Kerguelen Plateau: Cretaceous plateau volcanism in the southeast Indian ocean. Chemical Geology 120, 315–345.
Mahoney, J.J., Sheth, H.C., Chandrasekharam, D., Peng, Z.X., 2000. Geochemistry of flood basalts of the Toranmal section, northern Deccan traps, India: implications for regional Deccan stratigraphy. Journal of Petrology 41, 1099–1120.
Mallikharjuna Rao, J., 2002. Petrology and geochemistry of dolerite dykes, West Garo Hills Meghalaya – a preliminary study. Gondawana Research 5, 884–888.
McDonough, W.F., Sun, S.-S., 1995. The composition of the Earth. Chemical Geology 120, 223–253.
McDonough, W.F., Sun, S.-S., Ringwood, A.E., Jagoutz, E., Hofmann, A.W., 1992. K, Rb and Cs in the earth and moon and the evolution of the earth's mantle. Geochimica et Cosmochimica Acta 56, 1001–1012.
Melluso, L., Beccaluva, L., Brotzu, P., Gregnanin, A., Gupta, A.K., Morbidelli, L., Traversa, G., 1995. Constraints on the nature of the mantle sources of Deccan traps from the petrology and geochemistry of the basalts of Gujarat state (western India). Journal of Petrology 36, 1393–1432.
Melluso, L., Sethna, S.F., Morra, V., Khateeb, A., Javeri, P., 1999. Petrology of the mafic dyke swarm of the Tapti river in the Nandurbar area (Deccan Volcanic Province). Memoir Geological Society of India 43, 735–755.
Melluso, L., Srivastava, R.K., Petrone, C.M., Guarino, V., Sinha, A.K., 2012. Mineralogy and magmatic affinity of the Jasra clinopyroxenitic-gabbroic-syenitic complex, Shillong plateau, Northeastern India. Mineralogical Magazine 76, 1099–1117.
Misra, S., 2006. Precambrian chronostratigraphic growth of Singhbhum-Orissa craton, eastern Indian shield. Journal of the Geological Society of India 67, 356–378.
Misra, K.S., 2008. Dyke swarms and dykes within the Deccan volcanic province, India. In: Srivastava, R.K., Sivaji, C., Chalapathi Rao, N.V. (Eds.), Indian Dyke: Geochemistry, Geophysics and Geochronology, Narosa Publishing House Pvt Ltd, New Delhi, pp. 57–72.
Mohr, P.A., 1987. Crustal contamination in mafic sheets: a summary; In: Halls, H.C., Fahrig, W.F. (Eds.), Mafic Dyke Swarms. Geological Association of Canada Special Paper 34, 75–80.
Mukhopadhyay, D., 1988. Precambrian of the eastern Indian shield. Memoir 8, Geological Society of India, Bangalore.
Murthy, N.G.K., 1987. Mafic dyke swarms of the Indian shield. In: Halls, H.C., Fahrig, W.F. (Eds.), Mafic Dyke Swarms. Geological Association of Canada Special Paper 34, 393–400.
Naqvi, S.M., Rogers, J.J.W., 1987. Precambrian Geology of India. Oxford University Press, Oxford.
Naqvi, S.M., Divakar Rao, V., Narain, H., 1974. The protocontinental growth of the Indian Shield and the antiquity of its rift valleys. Precambrian Research 1, 345–398.
Parker, A.J., Rickwood, P.C., Tucker, D.H., 1990. Mafic Dykes and Emplacement Mechanisms. A.A. Balkema, Rotterdam.
Patil, S.K., Arora, B.R., 2008. Palaeomagnetic and rock magnetic studies on the intrusive from Raniganj basin, Damodar valley: linkage to the Rajmahal volcanic. In: Srivastava, R.K., Sivaji, C., Chalapathi Rao, N.V. (Eds.), Indian Dyke: Geochemistry, Geophysics and Geochronology, Narosa Publishing House Pvt Ltd, New Delhi, pp. 511–526.
Paul, D.K., 2005. Petrology and geochemistry of the Salma dike, Raniganj coalfield Lower Gondwana), eastern India: linkage with Rajmahal or Deccan volcanic activity? Journal of Asian Earth Sciences 25, 903–913.
Pearce, J.A., Cann, J.R., 1973. Tectonic setting of basic volcanic rocks investigated using trace element analysis. Earth and Planetary Science Letters 19, 290–300.

Pringle, M.S., Storey, M., Wijbans, J., 1994. 40Ar/39Ar geochronology of Mid-Cretaceous Indian Ocean basalts: constraints on the origin of large flood basalt provinces. EOS Transactions American Geophysical Union 75 (abstract).
Radhakrishna, T., Gopakumar, K., Murali, A.V., Mitchell, J.G., 1991. Geochemistry and petrogenesis of Proterozoic mafic dykes in north Kerala, southwestern Indian shield—preliminary results. Precambrian Research 49, 235–244.
Ramakrishnan, M., Vaidyanadhan, R., 2010. Geology of India. Geological Society of India, Bangalore.
Ray, J.S., Ramesh, R., Pande, K., 1999. Carbon isotopes in Kerguelen plume-derived carbonatites: evidence for recycled inorganic carbon. Earth and Planetary Science Letters 170, 205–214.
Ray, J.S., Trivedi, J.R., Dayal, A.M., 2000. Strontium isotope systematics of Amba Dongar and Sung Valley carbonatite–alkaline complexes, India: evidence for liquid immiscibility, crustal contamination and long-lived Rb/Sr enriched mantle source. Journal of Asian Earth Sciences 18, 585–594.
Ray, R., Sheth, H.C., Mallik, J., 2007. Structure and emplacement of the Nandurbar-Dhule mafic dyke swarm, Deccan Traps, and the tectonomagmatic evolution of flood basalts. Bulletin of Volcanology 69, 531–537.
Rollinson, H.R., 1993. Using geochemical Data: Evaluation, Presentation, Interpretation. Longman, Essex.
Rudnick, R.L., Fountain, D.M., 1995. Nature and composition of the continental crust: a lower crustal perspective. Reviews of Geophysics 33, 267–309.
Salters, V.J.M., Storey, M., Sevigny, J.H., Whitechurch, H., 1992. Trace element and isotope characteristics of Kerguelen Plateau region. Proceedings Ocean Drilling Progress, Science Results 120, 55–62.
Sarkar, A., Datta, A.K., Poddar, B.C., Kollapuri, V.K., Bhatacharya, B.K., Sanwal, R., 1996. Geochronological studies of Mesozoic igneous rocks of eastern India. Journal of Southeast Asian Earth sciences 13, 77–81.
Sharma, R.S., 2009. Cratons and Fold Belts of India. Springer–Verlag, Heidelburg.
Srivastava, R.K., 2011. Dyke Swarms: Keys for Geodynamic Interpretation. Springer–Verlag, Heidelburg.
Srivastava, R.K., Ahmad, T., 2008. Precambrian Mafic Magmatism in the Indian Shield – Part I. Journal of the Geological Society of India, Bangalore 72 (1) (Special Issue).
Srivastava, R.K., Ahmad, T., 2009. Precambrian Mafic Magmatism in the Indian Shield – Part II. Journal of the Geological Society of India, Bangalore 73 (1) (Special Issue).
Srivastava, R.K., Singh, R.K., 2004. Trace element geochemistry and genesis of the Precambrian sub-alkaline mafic dykes from central India craton: evidence for mantle metasomatism. Journal of Asian Earth Sciences 23, 373–389.
Srivastava, R.K., Sinha, A.K., 2004a. Early Cretaceous Sung Valley ultramafic–alkaline–carbonatite complex, Shillong Plateau, Northeastern India: petrological and genetic significance. Mineralogy and Petrology 80, 241–263.
Srivastava, R.K., Sinha, A.K., 2004b. Geochemistry and petrogenesis of early Cretaceous sub-alkaline mafic dykes from Swangkre-Rongmil, East Garo Hills, Shillong plateau, Northeast India. Earth and Planetary Sciences (Proceedings of the Indian Academy of Sciences) 113, 683–697.
Srivastava, R.K., Sinha, A.K., 2007. Nd and Sr isotope systematics and geochemistry of plume related early Cretaceous alkaline–mafic–ultramafic igneous complex from Jasra, Shillong Plateau, Northeastern India. Geological Society of America Special Paper 430, 815–830.
Srivastava, R.K., Heaman, Larry.M., Sinha, A.K., Shihua, S., 2005. Emplacement age and isotope geochemistry of Sung valley alkaline–carbonatite complex, Shillong Plateau, Northeastern India: implications for primary carbonate melt and genesis of the associated silicate rocks. Lithos 81, 33–54.
Srivastava, R.K., Sivaji, C., Chalapathi Rao, N.V., 2008a. Indian Dykes: Geochemistry, Geophysics and Geochronology. Narosa Publishing House Pvt Ltd, New Delhi.
Srivastava, R.K., Sivaji, C., Chalapathi Rao, N.V., 2008b. Indian dyke through space and time: Retrospect and prospect. In: Srivastava, R.K., Sivaji, C., Chalapathi Rao, N.V. (Eds.), Indian Dyke: Geochemistry, Geophysics and Geochronology, Narosa Publishing House Pvt Ltd, New Delhi, pp. 1–18.
Srivastava, R.K., Chalapathi Rao, N.V., Sinha, A.K., 2009. Cretaceous alkaline intrusives with affinities to aillikites from the Jharia area: magmatic expression of metasomatically veined and thinned lithospheric mantle beneath the Singhbhum Craton, Eastern India. Lithos 112, 407–418.
Srivastava, R.K., Ernst, R., Hamilton, M.A., Bleeker, W., 2010. Precambrian large igneous provinces (LIPs) and their dyke swarms: new insights from high-precision geochronology, paleomagnetism and geochemistry. Precambrian Research 183 (3) (Special Issue).
Srivastava, R.K., Sinha, A.K., Kumar, S., 2012. Geochemical characteristics of Mesoproterozoic metabasite dykes from the Chotanagpur Gneissic Terrain, eastern India: implications for their emplacement in a plate margin tectonic environment. Journal of Earth System Sciences 121, 509–523.
Storey, M., Kent, R.W., Saunders, A.D., Hergt, J., Salters, V.J.M., Whitechurch, H., Sevigny, J.H., Thirlwall, M.F., Leat, P., Ghose, N.C., Gifford, M., 1992. Lower Cretaceous volcanic rocks on continental margins and their relationship to the Kerguelen Plateau. Proceedings Ocean Drilling Progress, Science Results 120, 33–53.
Sun, S.-S., 1980. Lead isotopic study of young volcanic rocks from midocean ridges, ocean island and island arcs. Philosophical Transaction of Royal Society of London A297, 409–445.
Tarney, J., Weaver, B.L., 1987. Geochemistry and petrogenesis of early Proterozoic dyke swarms. In: Halls, H.C., Fahrig, W.F. (Eds.), Mafic Dyke Swarms. Geological Association of Canada Special Paper 34, 81–94.
Tatsumi, Y., Eggins, S.M., 1995. Subduction Zone Magmatism. Blackwell, Oxford.
Verma, S.P., Torres-Alvarado, I.S., Sitelo-Rodriguez, Z.T., 2002. SINCLAS: Standard igneous norm and volcanic rock classification system. Computer Geosciences 28, 711–715.
Weaver, B.L., Tarney, J., 1984. Estimating the composition of the continental crust: an empirical approach. Nature 310, 575–577.
White, R.W., McKenzie, D.P., 1989. Magmatism at rift zones: the generation of volcanic continental margins and flood basalts. Journal of Geophysical Research 94, 7685–7729.
Zhao, J.H., Zhou, M.F., 2007. Geochemistry of Neoproterozoic mafic intrusions in the Panzhihua district (Sichuan Province, SWChina): implications for subduction-related metasomatism in the upper mantle. Precambrian Research 152, 27–47.